

APR 14 1943

~~11~~
~~11~~
~~11~~



TECHNICAL MEMORANDUMS
NATIONAL ADVISORY COMMITTEE FOR AERONAUTICS

No. 1043

EXPERIMENTAL INVESTIGATION OF A MODEL
OF A TWO-STAGE TURBOBLOWER
By S. Dovjik and W. Polikovsky
Central Aero-Hydrodynamical Institute

Straight Through

Approved for
the Bureau of
Aeronautics
Laboratory.

Washington
April 1943



3 1176 01441 5047

NATIONAL ADVISORY COMMITTEE FOR AERONAUTICS

TECHNICAL MEMORANDUM NO. 1043

EXPERIMENTAL INVESTIGATION OF A MODEL

OF A TWO-STAGE TURBOBLOWER*

By S. Dovjik and W. Polikovsky

SUMMARY

In the present paper an investigation is made of two stages of a multistage turboblower having a vaneless diffuser behind the impeller and guide vanes at the inlet to the next stage. The method employed was that of investigating the performance of the successive elements of the blower (the impeller, vaneless diffuser, etc.) whereby the kinematics of the flow through the blower could be followed and the pressure at the different points computed. The character of the flow and the physical significance of the loss coefficients could thereby be determined so as to secure the best agreement of the computed with the actual performance of the blower. Since the tests were carried out for various delivery volumes, the dependence of the coefficients on a number of factors (angle of attack, velocities, etc.) could be obtained. The distribution of the losses that occur during the transformation of dynamic pressure at the impeller exit into static pressure could be found and likewise the range within which the friction coefficient varies in the vaneless diffuser. With the aid of factors having a certain physical significance, the centrifugal blower could be computed on the basis of a more or less schematical consideration of the phenomena occurring during the air flow through it, and the use of arbitrary factors and recourse to the geometrical similitude law thus avoided. The present investigation largely summarizes all the previous work of the CAHI Blower Section on the different elements of a centrifugal blower. Some considerations on the analysis of model test data for application to full-scale are presented in the appendix.

*Report No. 191 of the Central Aero-Hydrodynamical Institute, Moscow, 1935.

I. GENERAL

INTRODUCTION

The present methods of computation of blowers by a study of the successive elements, in particular the method applied at CAHI, permits, by introducing correction loss coefficients, the determination of the pressure at the blower outlet for given inlet conditions as well as the pressures at all transition points of the blower. The study of the pressures at these points - at the impeller outlet, guide vane inlet and outlet, and the various stage outlets - at various air deliveries is of great interest. On the one hand, it permits checking the correctness of the computation method itself and its correspondence to the physical nature of the phenomena occurring in the machine and, on the other hand, makes it possible directly from the test to determine such values of the loss coefficients as will assure the best agreement of the computed and actual performance data of the machine.

The direct measurement of the pressures at the various points of a centrifugal machine presents extremely great difficulty both of a technical and especially of a theoretical order. The pressure immediately behind the impeller, the correct determination of which is the fundamental problem in the computation of any centrifugal machine, may be correctly determined only for the case where the measuring apparatus rotates together with the impeller. Otherwise, that is, measuring at a stationary setting, the pressure is obtained in a region of unstable flow with respect to time and which by its very nature partakes of the periodic character of the flow.*

*The nonuniformity of the velocities and pressures between the blades of the impeller should arise not only in connection with the phenomenon of flow separation from the blade walls but also in connection with the character of the phenomenon itself of imparting power to the air by an impeller. The presence of Coriolis forces acting on the blade and giving rise to a moment on the shaft corresponds to the difference in pressures and velocities at the two sides of the blade. In its most general form this result follows directly from the hydrodynamic consideration that the increase in the total pressure at any
(Continued on p. 3)

Notwithstanding their extreme complexity, investigations of such type are possible and their results have appeared in various papers. Those by Thoma, Hagmayer and others (reference 1), while very important from the point of view of the direct investigation of the structure of the flow through the impeller, admit of a number of negative characteristics which made it necessary to dispense with the method in setting up our present investigation.

The first reason, though not the principal one, for not investigating the pressures behind the impeller with the aid of measuring apparatus rotating together with the impeller is the extreme complexity of such investigations. The preparation of the impeller model, the complicated internal communication system, the necessity for complete hermetic sealing make such investigations extremely laborious and lead to the result that the investigation of a single operating condition of any impeller is transformed into a complicated problem in scientific method. The given investigation, however, is more typical in its procedure and one of its main advantages is that, standing between a whole series of previous and subsequent investigations, it makes possible much greater reliability in evaluating the obtained results by their relative comparison.

The second and fundamental reason for not employing the direct measurement of the pressures at the various points of the model at its rotating and stationary parts in the casing is that the structural elements of any fan consist of relatively short curvilinear passages in which an unstable flow occurs. The determination of the directions and magnitudes of the velocities under these conditions, though possible; presents great experimental difficulties. As regards the measurement of the static pressures in such flow, it may be stated that with our present

(Continued from p. 2)

point of the flow through the impeller is determined from the equation

$$\frac{dH}{dt} = \frac{dP}{dt}$$

i.e., the necessary condition for the possibility itself of increasing the pressure is change with respect to time of the pressure at any point lying within the impeller.

state of measuring technique to carry out such measurements with any degree of accuracy is impossible particularly if account is taken of the specific character of the performance of the centrifugal machine in which dynamic pressures usually constitute a considerable fraction of the pressures measured.

The experience of a large number of investigators who have studied the flow of fluids in curvilinear channels (reference 2) has shown the very great value of studying the pressures and velocities at various points of the channel for the analysis of the flow phenomena. The same experience has also shown, however, that all these investigations cannot be used as a basis for computing the resistances due, on the one hand, to their insufficient accuracy and, on the other, to the extreme complexity of the picture obtained. The resistance of curved channels and channels of variable cross section practically must be investigated by considering them blower elements. By mounting at the channel inlet and outlet a rectilinear portion of sufficient length serving to equalize the field and to obtain a stabilized flow we are enabled, by measuring the pressure at two points, to obtain the loss coefficients, required for practical computations, of the elements under consideration. In certain cases, when the presence of the equalizing channel ahead of or behind the element under consideration does not correspond to its normal operating conditions, the equalizing channels, one or both, are replaced by measuring chambers. Thus, the measurement of the pressure at only two points may be required for determining the resistance of the element under consideration.

The fundamental principle of the methods of investigation therefore consists in creating inlet and outlet conditions for which the determination of the total pressure offers no special difficulties. Evidently the resistance of the element is the difference between the pressures at its inlet and outlet. This is the principle which has been taken as a basis of the investigation presented below of a turboblower model. The setting up of a definite pressure at the exits of the stages under consideration was effected by discharging the air directly into the atmosphere, as shown by the sketches in figure 1. The dynamic pressure at the outlet of the impeller may be found by investigating the kinematics of the flow essentially determined by the power imparted to the air. The dynamic pressure at the outlet of the guide vanes is determined from the condition that the outlet section is

filled out and from the pressure at the outlet. The dynamic pressure at the outlet from the stage is likewise determined from the condition of filling out of the cross section. As will be shown below, the equation of continuity, that is, the condition that the above-mentioned sections are filled out, may be used with sufficient justification.

During the experiment the pressure behind the element was held constant and equal to the atmospheric pressure. The pressure in the chamber ahead of the blower was varied, that is, the blower worked on suction. By taking the pressure in the chamber as the zero point of the computations, we may, with the aid of the above considerations, obtain the mean pressure behind the blower element. Knowing, in addition, the mean dynamic pressure in the element, we obtain the value of the total pressures in sections a-a, b-b, and c-c (fig. 2). At section o-o at the entrance to the blower the total pressure is taken equal to zero.

By comparing the change in the total pressure in passing from one section to another with the theoretical, we can determine the losses in the blower element. The characteristics of all the stages as well as those of the individual elements (fig. 1), that is, the curves of pressure H_{st} against volume Q for the entire range of operation from $Q = 0$ to $H_{st} = 0$ and $Q = Q_{max}$ permits the determination of the losses as a function of the flow kinematics and the extent of agreement of our assumed computation scheme with the actual phenomena.

A certain reservation in our computation method should be noted, namely, that the principle of direct summation of the successive individual resistances should be considered as only a first approximation. The local hydraulic resistances, which affect the very nature of the flow, certainly produce an effect on the succeeding resistances and in some cases greatly modify the values of the corresponding coefficients. The interference effect of the successively connected resistances was studied in the papers of Kirchbach and of Schubart (reference 3) who investigated the total resistance coefficient of two elbows as a function of the length of the straight portion between them. Both of these papers bring out with sufficient clearness the fact that considering the complex resistance of any system as equal to the sum of the

resistances of each of the elements that enter the system, that is, not taking account of the mutual interference between them, a value for the resistance is obtained that deviates by a considerable amount from the true value. Nevertheless this method of computation is the one generally employed in practice. This is explained by the fact that the method appears to be the only one that permits, even approximately, the determination of the resistances in making a new design. The degree of accuracy of such a provisional method will evidently be greater the more nearly the operating conditions of each of the elements included approach the conditions at which their resistances are directly determined. It is extremely difficult to determine technically a suitable degree of approximation of the test conditions of the blower elements to those conditions under which the elements actually operate and for which the computation is conducted. With respect to this question there are a large number of opinions held that express the most varied points of view.

On the one hand, a large number of turbomachine works (Brown-Boveri and Metro-Vickers) and likewise many investigators (Rateau, German, and Fedorov) consider the blower computation by the method of similitude as the only suitable one. This corresponds to assuming such strong mutual influence between the work of the individual blower elements that the combination is considered as a strongly unified system not subject to decomposition into its component elements. On the other hand, a large number of hydraulic engineers and hydrodynamicists (Kearton, Pfleiderer, and Gibson) and many production works (Electrocil and General Electric) hold a different point of view and assume that in practical computations it is permissible to make use of the resistance coefficients obtained in studying the stationary models.

Our point of view in this matter is that the machine may be divided up into elements the computation and investigation of each of which may lead, as has already often been the case, to sufficiently close agreement between the computed and test results. Two fundamental conditions should, however, here be considered: (1) the individual elements should be studied under conditions sufficiently near those at which the elements operate in the machine and (2) the study of the elements should be conducted not in the order of single, interrupted experiments but in the order of their systematic study. Only in this way may a definite idea of the effect of changing

the fundamental geometric or kinematic parameters on the work of the elements be obtained and this in turn permits them to be introduced in the computation under operating conditions differing from the test conditions.

It must be admitted that the computation by similitude considerations, that is, the method of projecting new designs with the aid of nondimensional characteristics obtained from experiment, is the most reliable method and can be depended on by the constructor not to give unexpected, disagreeable results. At the same time, by its very nature this method is a "reactionary" one that hinders further technical development. Moreover, in solving the problem of the design of new machine types under given conditions with the aid of nondimensional characteristics, it is necessary in very many cases to admit solutions known to be nonoptimum since no amount of previously produced and tested machines could cover entirely the broad range of modern high-speed machines. Furthermore, this fundamentally most reliable method of projecting a design from existing data instead of making a new computation leaves the designer entirely "disarmed" in those cases where a specific requirement in size or design makes it necessary for him to depart from the "canonical" shape. The strong tendency of modern machine construction; namely, the organic inclusion of auxiliary systems (fans, pumps, superchargers of aviation engines, etc.) does not permit, in very many cases, making use of the method of computation from existing data and makes necessary the computation of the machine taking into account marked individual conditions of mounting, construction, and utilization.

The problem of the general investigation of the internal process of centrifugal machines over a wide range of delivery volumes and pressures is one of great importance under our conditions of a planned socialist economy. In designing blowers for a single definite operating condition, it is possible to choose profiles and sections based on considerations of smoothest flow of the fluid through the machine. With a relatively limited range of correction coefficients corresponding to the optimum conditions, it is possible to design entirely satisfactory machines intended to work at a single operating condition. At the same time, however, each turbomachine has a more or less wide range of application in connection with the more or less level range of its efficiency curve near the maximum. The above-mentioned

method of computing the machine for only a single operating condition gives no indication, however, of its range of possible application. Under the conditions prevailing in Soviet Russia the design of individual machines is becoming more and more a rare phenomenon. In the majority of cases systems are designed which are used for series or even mass production. For those machines put out in series and not for individual requirements, the question of the range of possible application is a very acute one. In connection with this question it is necessary, in designing a machine, to determine by preliminary computation its data not only for a single operating condition but, at least with a certain approximation, to construct the various parts of the characteristic curves. In such a computation the considerable deviation of the flow at various points from the corresponding optimum hydraulic conditions must be taken into account. For this purpose a knowledge of the work of the individual elements over a wide range of entry angles, velocities, and so forth, is necessary. The work presented below is based on just this consideration.

DESCRIPTION OF TESTS

For the object of the investigation a two-stage turboblower model was chosen (fig. 3). As may be seen from the aerodynamic scheme shown, the impellers of the first and second stages, for the same inlet and outlet diameters D_0 and D_2 , respectively, of the impeller, had different inlet diameters to the blades D_1 (for the impeller of the first stage the blades were somewhat shortened). Moreover, the impellers differed from each other also in the inlet and outlet angles and in the impeller width (figs. 4a and 4b).

The test was conducted in the laboratory of the CAHI Blower Section in the suction chamber shown in figure 5. The distinguishing feature of this chamber as compared with other low pressure chambers is the presence of an additional blower the output of which is entirely or partially used to make up for all resistances of the chamber itself and pipes. Due to this fact it was possible to obtain points on the characteristic for resistances equal to zero or near this value. As may be seen from the layout of the chamber (fig. 6) the air delivery was determined with the aid of a conical collector placed in the

chamber. In obtaining the characteristics of the blower in this chamber, the air delivery was usually measured with a pitot tube located at the entrance part of the chamber. Taking account, however, of the relatively large pressures produced by the blower (above 200 mm water) and the resulting danger of leakage that might impair the characteristics, it was necessary to measure the air delivery with the aid of a collector.

This method of determining the amount of gas flowing through the blower is based on the fact that in testing a centrifugal machine for suction at any section a lowering in pressure is formed equal in magnitude to the dynamic pressure of the flowing gas plus the losses over the path from the entrance to the place of measurement. Thus, the equation of Bernoulli, written for the cross sections through the tubes measuring the general suction in the chamber (sec. I) and the suction in the collector (sec. II) is

$$h_{\text{cham}} + \rho \frac{v_1^2}{2} = h_{\text{imp}} + \rho \frac{v_2^2}{2} + \Delta h$$

The velocity in section I due to the relatively large dimensions of the suction chamber is so small that it may, without any appreciable error, be neglected.

Hence

$$h_{\text{cham}} - h_{\text{imp}} = \rho \frac{v_2^2}{2} + \Delta h$$

By estimating the losses over the path from the entrance to the collector to the point of measurement (in our case this distance was equal to a diam.) as 3 to 4 percent, we obtain

$$\rho \frac{v_2^2}{2} = 0.96 (h_{\text{cham}} - h_{\text{imp}})$$

As may be seen from the test setup, the velocity head h_{dyn} is obtained as the difference between the suction in the collector and the total suction in the chamber.

The amount of air flowing through the labyrinth packing was not specially measured, since the computations showed that the magnitude of this leakage constitutes in all only 2 to 3 percent of the total air delivery, that is, lies within the range of experimental accuracy.

The power required by the blower was measured on a balancing stand by determining the turning moment obtained by the motor. It should be noted that the turning moment of the motor is equal to the sum of the moments required in turning the impellers and in overcoming the friction in the bearings. For this reason, a preliminary determination of the friction moment for a given rotational speed made possible in a further experiment the direct determination of the power required by the impeller.

The operating conditions were varied with the aid of a throttle located at the exit section of the blower and also by the change in the rotational speed of the blower.

In correspondence with the general method, discussed above, underlying our experiment, of investigating the work of the individual elements of the turboblower (isolated impeller, guide vanes, etc.) the characteristic curves of H , N , and η against Q were successively obtained. This made it possible to analyze the phenomena in each of the turboblower elements, eliminating from consideration those phenomena which occur simultaneously in the other elements of the blower. The test was thus reduced to obtaining the following series of characteristics:

- (a) Isolated impeller of the first stage (fig. 7a)
- (b) Isolated impeller of the second stage (fig. 7b)
- (c) Impeller of the first stage together with the vaneless diffuser behind the impeller (fig. 8a)
- (d) Same for the second stage (fig. 8b)
- (e) First stage of the blower including the impeller, vaneless diffuser, and guide vanes (fig. 9a)
- (f) Same for the second stage (fig. 9b)

II. ANALYSIS OF TEST DATA.

The basic data in investigating the work of the blower, as has been said above, were the test characteristics obtained. The latter consist of the two curves of the static pressure H_{st} and power expended N against the air volume Q . Their analysis consisted in comparing the test curves obtained with those computed and determined by methods worked out at CAHI for the computation of centrifugal machines. The method of determining the various magnitudes entering the computation is the one given below.

1. Theoretical Pressure Developed by the Impeller

The power N expended by the blower is made up of the sum of (a) the useful (hydraulic) power N_h imparted to the active flow of the air and directly used for developing pressure and overcoming the hydraulic resistances and (b) the power N_o expended in friction at the surfaces of the impeller and production of turbulent flow.

The magnitude N_o may, with sufficient degree of accuracy, according to numerous investigations of the Blower Section, be assumed as a constant magnitude, independent of the discharge and equal to the power loss at $Q = 0$. This magnitude, which is fundamentally a function of the diameter of the impeller, its width and the degree of roughness of its surfaces, may be computed by the formula

$$N_o = \beta \rho \omega^3 D^5 \left(1 + 5 \frac{b}{D} \right)$$

The coefficient β entering the above formula, according to the data of Stodola, Pfleiderer, CAHI, and others (reference 4), is $(2-3) 10^{-6}$ for smooth solid disks. In the investigation of impellers of centrifugal blowers conducted by V. Polikovskiy (reference 5), the value of this coefficient varied between $(20-25) 10^{-6}$. Our tests gave the value $\beta = (12-16) 10^{-6}$. Approximately the same values for β were obtained from the results of tests on a number of impellers that were conducted at the CAHI Blower

Section. The deviations in the values of this coefficient obtained by us from data used in the work of V. Polikovskiy may be explained by the very great roughness of the plane parallel shape of the impeller series tested by him.

It must nevertheless be admitted that the value of the coefficient β obtained in the tests of centrifugal impellers are considerably greater than the value of the same coefficient for smooth solid disks. Tests are, at the present time, being conducted at the Blower Section on the effect on the power N_0 expended in friction of the shape of the impeller (flat and semiconical), the type of blades, the presence of disks, and other factors.

The difference between the power N directly measured on the balancing stand and the power N_0 expended in friction is the hydraulic power N_h directly used in developing the pressure and overcoming the hydraulic losses

$$N_h = N - N_0 \quad (1)$$

In the further analysis of the data, the value of the hydraulic power was taken for each impeller as the mean of three of its values used in obtaining the characteristics: the isolated impeller, the impeller with vaneless diffuser, and complete stage. (See figs. 10a and 10b.)

From the Euler equation

$$H_{th} = \rho C_{2u} U_2 \quad (2)$$

we can obtain the expression

$$N_h = \frac{Q_{sec} H_{th}}{75} = \frac{Q_{sec} \rho C_{2u} U_2}{75}$$

by which, for a given initially determined hydraulic power N_h , the rotational velocity of the flow behind the impeller C_{2u} (the tangential component of the absolute velocity at the exit) is readily determined:

$$C_{2u} = \frac{75 N_h}{\rho Q_{sec} U_2} \quad (3)$$

and the total head (theoretical) produced by the impeller

$$H_{th} = \rho C_{2u} U_2 \quad (4)$$

The values of the total pressures obtained are given in table 1.

2. Investigation of the Impeller of the Turboblower

Having determined the value of the theoretical pressure that can be developed by the impeller of the turboblower, we pass on to an analysis of the phenomena that occur in the impeller. The problem which we now consider consists, on the one hand, of an explanation of the kinematics of the flow through the impeller and, on the other hand, an explanation of the character and magnitude of the losses that are involved.

a) Character of the flow at inlet to the impeller blades. - The flow enters the impeller in the axial direction with an inlet velocity C_0 (fig. 11). The magnitude of this velocity for each operating condition may be determined from the equation of continuity

$$C_0 = \frac{Q_{sec}}{\mu F_0}$$

where F_0 is the useful inlet area, taking account of the presence of the shaft, special flows, and so forth, that decrease the inlet area; μ is the coefficient that takes into account the possibility of incomplete filling out of the inlet cross section. For single-stage machines with axial air entry $\mu = 1$; for the individual stages of a multi-stage machine, however, the value of this coefficient may be less than 1 depending on the smoothness of the deflection from one stage to the next, and so forth. In deflecting at the blades in the meridional plane by 90° this velocity undergoes a change associated with the contraction of the flow during deflection. For this reason, in determining

the magnitude of the meridional or radial component of the absolute inlet velocity to the impeller blades C_{1m} it is necessary to take into account the possibility of incomplete filling out of the impeller where the deflection occurs and the associated increase in the velocity after deflection by the introduction of a contraction coefficient μ .

The contraction of the flow was especially investigated in the laboratory of the Blower Section (reference 6), values of the coefficient μ , a function of the ratio D_1/D_0 , width b , smoothness of rounding at inlet, and so forth, being obtained within the range $\mu = 0.6-0.85$. It should be observed that this investigation was conducted on a stationary lattice and it is natural that the rotating impeller where the spread of the flow over the width of the impeller is extremely intensified the value of this coefficient should be raised. In particular cases when the inlet diameter to the blades D_1 is considerably greater than the inlet diameter to the impeller D_0 , as shown by the analysis of an entire series of impellers (reference 7), the flow at the diameter D_1 completely fills out the impeller section and μ becomes equal to unity. In analyzing our test data, the following values were taken for this coefficient: for the impeller of the first stage for which $D_1 = D_0$, $\mu = 0.9$; for the impeller of the second stage for which D_1 was greater than D_0 , $\mu = 0.98$. In this manner the magnitude of the radial component of the absolute inlet velocity C_{1m} was determined by the equation

$$C_{1m} = \frac{Q_{sec}}{\pi D_1 b_1 \mu} \quad (5)$$

A real fluid having viscosity obtains a certain rotational velocity due to the rotation of the impeller and that is taken into account by the coefficient of initial flow spin $\varphi_1 = C_{1u}/U_1$. As a special investigation has shown (reference 8), for a given impeller the value of this coefficient may, to a first approximation, be considered as a constant independent of the volume delivered (velocity of approach to the impeller). In his paper V. Polikovskiy gives the value of this coefficient within the range 0.3-0.4. A somewhat wider range of variation is given by Gibson (reference 9) whose value of φ_1 lies within the range 0.3-0.5.

In analyzing a number of tests on centrifugal blowers a very good agreement of experimental and computed results was obtained for $\varphi_1 = 0.35$ and therefore this value of the coefficient was assumed by us for the impeller of the first stage. For the impeller of the second stage for which the inlet diameter to the blades D_1 was considerably greater than the inlet diameter to the impeller D_1 and the possibility of flow rotation at the inlet to the blades was considerably greater than in the impeller of the first stage, the value of this coefficient was taken equal to 0.4.

From the velocity vector diagram at the inlet (fig. 12), we find that the relative velocity of the flow at the blades W_1 may be expressed by

$$W_1 = \sqrt{C_{1m}^2 + (1 - \varphi_1)^2 U_1^2} \quad (6)$$

On the other hand, the value of the relative inlet velocity to the blades cannot be less than its value determined from the condition of filling out of the impeller at the inlet (condition of continuity of flow):

$$W_1 = \frac{Q_{sec}}{(\pi D_1 b_1 \sin \beta_1 - \delta b_1 z)\mu} = \frac{Q_{sec}}{F_1} \quad (7)$$

From a comparison of these two values we may finally determine the relative inlet velocity to the blades W_1 as the greater of these two.

From the velocity diagram we may also determine the angle made by the flow direction with the blades for various deliveries, namely,

$$\sin (\beta_1)_{f1} = \frac{C_{1m}}{W_1} \quad (8)$$

where W_1 evidently is equal to the velocity relative to the blades and not the entrance velocity to the impeller blades. The difference between the angle $(\beta_1)_{f1}$ and the blade angle at the inlet $(\beta_1)_{b1}$ defines the angle of attack α :

$$\alpha = (\beta_1)_{f1} - (\beta_1)_{b1} \quad (9)$$

The above defined magnitudes characterizing the flow at the inlet to the impeller are given in table 2.

b) Character of the flow at the impeller outlet.- The fundamental problem in drawing the velocity vector diagram at the impeller outlet is that of the relation between the relative velocities at the inlet and outlet of the impeller. Numerous investigations conducted at CAHI have shown that for positive entry angles to the impeller blades, if the latter are curved backward or radial, the relative velocity in flowing through the impeller does not change, that is, that $W_2 = W_1$. A detailed justification for this assumption may be found in the work of V. Polikovskiy. (See reference 5.) Here we may limit ourselves to certain elementary considerations.

In flowing through the rotating impeller the flow does not completely fill out the cross section of the passage formed by the blades and together with the active part of the flow, which moves forward, a neutral region is created in which turbulence arises. A brilliant experimental confirmation of this fact has been obtained by photographing the flow through a centrifugal impeller pump at the Munich laboratory by K. Fischer and D. Thoma (reference 1) (fig. 13). As is known, in the rotation of a centrifugal wheel the static pressure in the passage between the blades increases according to the law

$$\Delta H_{st} = \frac{U_2^2 - U_1^2}{2g} \gamma + \frac{W_1^2 - W_2^2}{2g} \gamma$$

The losses incurred in flowing through the impeller are not taken into account here because (as will be shown below) the main part of these losses is associated with phenomena that arise at the flow entrance to the blades (impact, turbulence, etc.); the friction losses at the blades being small enough so that they may without great error be neglected. We assume that in the turbulence region there is no forward motion of the flow, that is, that the relative velocity within it is equal to zero. The increase in pressure within this region during the impeller rotation therefore is exclusively at the expense of the rotational velocity, that is, will be equal to

$$\Delta H_{st \ tr} = \frac{U_2^2 - U_1^2}{2g} \gamma$$

On the other hand, this vortex region should be in static equilibrium with the active part of the flow, the equilibrium necessarily being maintained along the entire boundary between the regions. This is possible only in the case that the pressure increases in the active part of the flow and in the turbulence region are equal to each other, that is, if

$$\Delta H_{st} = \Delta H_{st \ tr}$$

or in other words if $W_2 = W_1$ (reference 10).

We note again that the above considerations apply only to the cases of positive angles of attack where the vortex region is not closed (fig. 14). Conditions are otherwise as regards the relation between W_2 and W_1 for negative angles of attack. In this case the vortex region formed at the front wall of the blade is generally closed and the flow can spread along the channel section with the result that W_2 may be considerably less than W_1 (fig. 15). For this reason, for blower operating conditions with negative flow angles we applied the following method of determining W_2 .

From the value of the rotational component at the impeller outlet C_{2u} , determined from the hydraulic power (see above), and making use of the velocity diagram, we may write down a first equation for the determination of the relative velocity at the impeller outlet:

$$W_2 = \frac{U_2 - C_{2u}}{(\cos \beta_2)_{f1}} \quad (10)$$

A second equation may be obtained from the assumption that the minimum value of the relative velocity W_2 will be the value determined from the continuity equation:

$$W_2 = \frac{Q_{sec}}{\pi D_2 b_2 (\sin \beta_2)_{f1} - \delta b_2 z} \quad (11)$$

In both of these equations there enters the angle $(\beta_2)_{f1}$ formed by the direction of the flow. This angle may differ considerably from the outlet blade angle $(\beta_2)_{bl}$ due to the flow deflection (deviation of the outflowing stream from the direction of the exit edge of the blade). Solving these two equations by the trial and error method, we determine the magnitude and direction of the relative velocity W_2 at the impeller outlet.

It should be remarked that the values of W_2 thus determined are somewhat too small since the value of the area of the flow in equation (11) does not take account of the possibility of the formation between the blades at the impeller outlet of vortex regions that do not take part in the forward motion of the flow.

From the velocity vector diagram we can readily determine the radial component of the absolute velocity at the impeller exit:

$$C_{2m} = W_2 (\sin \beta)_{f1} \quad (12)$$

together with the value of the absolute velocity at the impeller exit:

$$C_2 = \sqrt{C_{2m}^2 + C_{2u}^2} \quad (13)$$

The magnitudes characterizing the flow condition at the impeller exit are given in table 3.

c) Determination of the general value of the losses in the impeller.— Having explained the character of the flow at the impeller exit, we may determine by computation the static pressure behind the impeller as the difference between the total (theoretical) pressure developed by the impeller $H_{th} = \rho C_{2u} U_2$ and the dynamic pressure

$\rho \frac{C_2^2}{2}$, both of these values being determined by computa-

tion:

$$H_{st \text{ comp}} = H_{th} - H_{dyn} = \rho C_{2u} U_2 - \rho \frac{C_2^2}{2} \quad (14)$$

The difference between the computed static pressure curve $H_{st \text{ comp}}$ and the experimental curve $H_{st \text{ exp}}$ gives us the total value of the hydraulic losses in the impeller:

$$\Delta H_{imp} = H_{st \text{ comp}} - H_{st \text{ exp}} \quad (15)$$

The results obtained are collected in table 4 and plotted in figures 16a and 16b.

d) Analysis of the impeller losses. - The value of the total losses in the impeller ΔH_{imp} is conveniently represented as the sum of two, to some extent independent, values:

(a) The losses in deflecting the flow at the blades
 ΔH_c

(b) The entry and flow losses through the impeller
 ΔH_w

It is natural to refer the first group of losses to the dynamic pressure of the flow velocity C_{1m} after deflection at the blades and to write them in the form

$$\Delta H_c = \xi_c \frac{C_{1m}^2}{2} \rho \quad (16)$$

The value of the coefficient ξ_c should first of all depend on the structural characteristics of the impeller (the smoothness of the deflection in entering the blades, the relation between the diam. D_1 and D_0 , etc.) and may with sufficient justification be assumed as constant, independent of the air delivery. According to the test results on a number of impellers obtained at the Blower Section, the value of this coefficient fluctuates within the range 0.1-0.5. This range of values may appear to be relatively wide but we must remember that the resistance

coefficient of stationary elbows, as the investigations of Nippert and other authors have shown, varies within a still wider range depending on the smoothness of the deflection.

Taking account of the small amount of contraction of the stream in deflecting against the blades, the smoothness of the deflection, and so forth, we assumed the minimum value of this coefficient for both impellers; for the impeller of the second stage for which D_1 was greater than D_0 and the contraction of the stream less the value assumed was 0.1; for the impeller of the first stage corresponding to a higher contraction of the stream the value assumed was 0.2.

We thus obtain the values of the losses in deflecting at the blades ΔH_c and the losses in the flow through the blades as the difference between the total losses in the impeller ΔH_{imp} and ΔH_c :

$$\Delta H_w = \Delta H_{imp} - \Delta H_c \quad (17)$$

The losses in the air flow through the blades may arise from two causes: In the first place, the losses associated with the formation of turbulence regions in the passages between blades and in the second place, the losses due to friction at the blade surfaces. The latter losses evidently constitute a very small part as compared with the losses associated with the turbulence formation because, first, the passages between the impeller blades are relatively short and the friction losses cannot play a large part and secondly, as has been shown above, the flow does not entirely fill out the cross sections between the blades, the velocity distribution along the cross section, due to the action of Coriolis forces not being symmetrical. In the third place, for almost all operating conditions, impact* occurs at the impeller inlet since shockless entry can occur only at a single defined operating condition of a given impeller. This impact gives rise

*In applying the term "impact at the blade" it should be observed that a certain latitude is assumed. Actually we do not have here the impact phenomenon associated with the loss of a part of the momentum at the blade but with the phenomenon of flow separation. We make use of this term, however, because, notwithstanding its insufficient accuracy, it is very widely prevalent in the technical literature.

to flow separation directly behind the entry edge of the blade and to the formation of intense turbulence regions. The losses associated with the turbulence are naturally predominant in the general balance of losses in the air flow through the impeller.

Having explained the nature of the losses that arise in flowing through the impeller, we proceed to the determination of the coefficient characterizing these losses. It is natural to refer these losses to the velocity head corresponding to the relative inlet velocity, the loss coefficient ξ_W being then given by the expression

$$\xi_W = \frac{\Delta H_W}{\rho \frac{W_1^2}{2}} \quad (18)$$

The value of this coefficient should depend on a number of factors associated with the structural characteristics of the impeller (number of blades, their length, etc.) and the operating conditions of the blower, the angle of attack α , the degree to which the passage between blades is filled by the active fluid, and so forth. As has been shown, the main part of the flow losses through the impeller depends on the angle at which the blades are attacked so that the coefficient should likewise depend mainly on the angle α . A detailed analysis of the tests on a series of centrifugal impellers by V. Polikovskiy (reference 7) has shown that the values of this coefficient vary within the relatively wide limits of 0.8 to 0.05 (the larger values for positive angles, and smaller for negative ones).

The results of an analysis of the test data on the blower impellers were represented on curves, the values of the coefficient ξ_W being plotted against α (fig. 17).

As may be seen, for both impellers almost identical curves were obtained. It is interesting to note that the determination in the laboratory of the Blower Section of the resistance of the stationary blade lattice gave almost the same dependence of the loss coefficient ξ_W on the angle of attack α , thereby confirming the picture of the flow phenomena in the impeller. The small values of the coefficient ξ_W for negative angles of attack as compared with the values for zero and positive angles are to be

particularly noted. The explanation for this face is to be found in the different character of the turbulence regions. Whereas positive and zero angles of attack are associated with the formation of open vortex regions communicating with the space behind the impeller, the negative angles of attack give rise to the formation of closed regions. (See figs. 14 and 15). Since the coefficient ξ_w , although referred to the inlet velocity, takes into account not only the entrance losses but also those arising during flow through the impeller blades, the character of this flow naturally affects the value of this coefficient.

The employment of the curve expressing the dependence of the coefficient ξ_w on the angle of attack α in the design and computation of turboblowers is not sufficiently convenient. For this reason we assumed it possible to divide the entire range of operating conditions from $Q = 0$ to Q_{max} roughly into three regions within each of which the value of ξ_w for both impellers may to a first approximation be considered as constant. These regions are the following: the first is that with large positive angles of attack ($\alpha > +4^\circ$); this region corresponds to small delivery volumes (underload). The second region is approximately that for shockless entrance to the blades ($+4^\circ > \alpha > -4^\circ$) and corresponding to discharges near the optimum. The third region, finally, corresponds to high discharges (overload) associated with large negative angles ($\alpha < -4^\circ$). Within each of these regions assumed mean values of the coefficient ξ_w were plotted as dotted curves, and as may be seen on figure 17, the deviation of the test curves from these mean values was found to be very slight. These mean values of the coefficient ξ_w used in determining the general values of the flow losses through the impeller ΔH_w were $\xi_w = 0.65$ for the first region ($\alpha > +4^\circ$), $\xi_w = 0.4$ for the second region ($+4^\circ > \alpha > -4^\circ$), and $\xi_w = 0.1$ for the third region ($\alpha < -4^\circ$).

*The small values of the coefficient ξ_w obtained for large negative angles of attack may give an indication of the suitability of operation of the turboblowers at conditions corresponding to these angles. It should be noted that (1) operating conditions corresponding to large negative angles of attack correspond, for most of the impellers, (Continued on p. 23)

Substituting the assumed values of the coefficient ξ_W in the expression for the losses in flowing through the impeller:

$$\Delta H_W = \rho \frac{W_1^2}{2} \xi_W \quad (19)$$

we obtain the values of these losses. We can then determine by computation the value of the static head at the impeller outlet:

$$H_{st \text{ comp}} = H_{th} - H_{dyn \text{ comp}} - \Delta H_c - \Delta H_W \quad (20)$$

The results obtained are collected in table 5 and plotted on figure 18. It is quite evident that by taking for each delivery volume the corresponding value of the coefficient ξ_W from the curve of $\xi_W = f(\alpha)$ we would obtain complete agreement of the computed curves with the experimental ones.

The analysis of two impellers with different diameter of entrance to the blades D_1 for the same diameters of inlet and outlet of the impeller D_0 and D_2 permits us incidentally to make an interesting comparison and draw conclusions as regards the performance of such impellers (the first stage impeller for which $D_0 = D_1$ we shall denote as the normal, while the impeller of the second stage for which $D_1 > D_0$ we shall denote as the impeller with shortened blades).

(Continued from p. 22)

to conditions considerably above the design (optimum) operating conditions and are at the extreme right of the characteristic curve where even a slight change in the delivery is associated with relatively large changes in pressure; (2) notwithstanding the small values of the coefficient ξ_W the absolute value of the losses in flowing through the impeller ΔH_W corresponding to large deliveries constitute a considerable part; and (3) to operating conditions with negative angles of attack there corresponds an extremely unstable and undefined character of the vortex region.

(a) The jet contraction for the impeller with shortened blades is less than for the impeller with normal blades as a result of which the coefficient of flow contraction in deflection at the blades μ for the first stage is less than that for the second.

(b) The possibility of an initial rotation of the jet in flowing toward the blades in the case of the impeller with shortened blades is greater than for the normal impeller because the coefficient of initial rotation φ for the first stage impeller was found to be less than for the second stage impeller.

(c) The loss coefficient for the jet deflection at the blades ξ_c corresponding to the smaller jet contraction at the impeller with shortened blades was found to be less than for the second stage impeller.

(d) The flow loss coefficient through the impeller ξ_w was found to have almost identical values for the same angles of attack, thereby confirming the above assumption that the main part of the losses occurring in flowing through the impeller depends essentially on the angle of flow approach and is therefore a function of the angle α .

(e) In particular cases where there is a contracted entrance section and the relative inlet velocity to the impeller W_1 must be determined from the equation of continuity, it may be found convenient to shorten somewhat the blades at the impeller inlet (increase D_1). As a result the static head should increase at the expense of a decrease in the relative inlet velocity W_1 and since the losses, as is seen from the results of the above analysis, do not essentially change (and may even decrease somewhat at the expense of ΔH_c) the static efficiency may also increase. This is confirmed by the results of tests on a model of one of the LMZ blowers where, after shortening the blades somewhat, it was found possible to increase the static pressure of the impeller and the static efficiency (fig. 19).

3. Investigation of the Performance of the Vaneless Diffuser

The next stage in our blower investigation is an analysis of the performance of the vaneless diffuser.

A vaneless diffuser of constant width is constituted by two parallel planes which form a continuation of the impeller and are directly behind it (fig. 3). In the motion of the air flow from the impeller through the diffuser a partial transformation of the velocity head corresponding to the exit velocity from the impeller $\rho \frac{C_2^2}{2}$ into static pressure occurs.

If the losses through the diffuser are not taken into account the gain in static pressure in the diffuser would be

$$\Delta H_{st \text{ dif}} = \rho \frac{C_e^2}{2} - \rho \frac{C_a^2}{2}$$

where

C_e absolute flow velocity at the diffuser inlet

C_a absolute velocity at the diffuser outlet

Actually in the flow of the air through the diffuser losses occur the determination of which is the subject of the present part of our investigation.

The method given below of computing the losses in a vaneless diffuser is essentially that of Prof. O. Pfloiderer. (See reference 4.) A further development and simplification of this method with the object of facilitating its application to technical computations was obtained by V. Polikovskiy and M. Nevelson (reference 11) who, together with an analysis of the losses in the diffuser, presented a number of considerations in connection with the design of this element of the centrifugal blower. We shall therefore limit ourselves here to the consideration of the mode of operation of plane diffusers.

a) Character of the flow at entrance to the plane diffusers.— As a result of analysis of the performance of the impeller, all magnitudes have been determined which characterize the flow at the impeller exit: the absolute flow velocity C_2 and its components, namely, the tangential C_{2u} and meridional (radial) C_{2m} . Moreover we have determined the total head at the impeller outlet as the sum of the static head measured in the test $H_{st \text{ exp}}$

and the dynamic head $\rho \frac{C_2^2}{2}$ determined computationally.

We note that in the determination of the radial component of the impeller outlet velocity C_{2m} from the equation

$$C_{2m} = W_2 \sin (\beta_2)_{f1}$$

by introducing in the computation the flow exit angle $(\beta_2)_{f1}$ different from the blade exit angle $(\beta_2)_{b1}$ we take account of the deviation of the flow from the direction of the blades at exit and the possibility of incomplete filling of the impeller cross section along its width.

In entering a stationary element of the blower, such as the vaneless diffuser, the flow spreads along the entire width. Simplifying the phenomenon somewhat, we assume that this filling out of the diffuser over its width occurs instantaneously, that is, that at the inlet diameter D_3 in the diffuser equal to the outer diameter of the impeller D_2 the radial component C_{3m} may be determined from the continuity equation

$$C_{3m} = \frac{Q_{sec}}{\pi D_3 b_3} \quad (21)$$

The error which is here admitted in not taking account of the gradualness of the filling process is evidently negligible.

The value of the tangential component C_{3u} at the diffuser inlet is equal to the value of the velocity at the impeller outlet C_{2u} because the moment of momentum imparted to the flow by the impeller remains constant, that is,

$$C_{2u} = C_{3u} \quad (22)$$

From the values of these components of the absolute velocity C_{3m} and C_{3u} the absolute inlet velocity to the vaneless diffuser C_3 can be determined:

$$C_3 = \sqrt{C_{3m}^2 + C_{3u}^2} \quad (23)$$

and the angle at which the flow enters the diffuser

$$\tan \alpha_3 = \frac{C_{3m}}{C_{3u}} \quad (24)$$

(See table 6.)

b) Losses in the vaneless diffuser:

(1) Impact losses.- We have assumed above that a decrease in the radial component of the absolute velocity C_m from the value C_{2m} corresponding to the impeller outlet to the value C_{3m} corresponding to the diffuser inlet occurs instantaneously. During this instantaneous velocity change, the losses in the kinetic energy which lower the total pressure at the outlet may be computed by the theorem of Borda-Carno

$$\Delta H_{\text{impact}} = \rho \frac{(C_{2m} - C_{3m})^2}{2} \quad (25)$$

(2) Friction losses at the lateral surfaces of the vaneless diffuser.- The motion of the real fluid between the walls of the plane diffuser is associated with friction of the moving air at the lateral surfaces of the diffuser walls as a result of which the flow loses part of its total pressure head. For an element of path ds the friction loss is given by the following expression

$$dH_{\text{fr}} = \lambda \frac{ds}{4R_h} \rho \frac{C^2}{2}$$

where

λ friction coefficient depending essentially on the roughness of the diffuser walls

R_h hydraulic radius = $b/2$

that is,

$$dH_{fr} = \lambda \frac{ds}{2b} \rho \frac{C^2}{2} = \lambda \frac{ds}{2b} \rho \frac{C_m^2}{2} + \lambda \frac{ds}{2b} \rho \frac{C_u^2}{2} \quad (26)$$

It follows that the friction losses are made up of losses associated with the displacement of the flow in the radial and tangential directions.

In the radial direction the velocity head $\rho \frac{C_m^2}{2}$ cannot compensate the frictional losses, since the radial component at any section is determined by the cross-sectional area of the diffuser independently of the losses, and therefore the losses can evidently be covered only by the static head. In the tangential direction, however, the frictional losses will be covered by the rotational velocity head $\rho \frac{C_u^2}{2}$, that is, by a decrease in the magnitude of the latter.

Let us consider how the frictional losses affect the velocity C_u . The elementary power dN_r expended in overcoming the friction over a path element ds is given by

$$dN_r = dH_r Q_{sec} \frac{\text{kg}\cdot\text{m}}{\text{sec}} \quad (27)$$

The work of the frictional force dL in time dt will be

$$dL = dN_r dt = Q_{sec} dH_r dt \quad (28)$$

If this work occurs over the path element ds , the frictional force is

$$P = \frac{dL}{ds} = \frac{Q_{sec} dH_r dt}{ds} = Q_{sec} dH_r \frac{dt}{ds} \quad (29)$$

Substituting in the above equation the value found for the frictional losses dH_r , we obtain

$$P = \lambda Q_{sec} \frac{dt}{2b} \rho \frac{C^2}{2} \quad (30)$$

The moment of this force relative to the axis is

$$M_{\text{comp}} = \lambda Q_{\text{sec}} \frac{dt}{2b} \rho \frac{C^2}{2} l$$

where l is the lever arm equal to $R \cos \alpha = R \frac{C_u}{C}$. The moment of the frictional force about the axis is therefore

$$M_{\text{comp}} = \lambda Q_{\text{sec}} \frac{dt}{2b} \rho \frac{C^2}{2} R \frac{C_u}{C} = \rho Q_{\text{sec}} \frac{\lambda}{4b} RC_u C dt \quad (31)$$

The moment of the applied forces about the axis is equal to the change per second of the moment of momentum of the volume of fluid passing through, hence

$$M_{\text{comp}} = \rho Q_{\text{sec}} \frac{\lambda}{4b} RC_u C dt = \rho Q_{\text{sec}} R(dC_u) \quad (32)$$

whence the losses of the tangential component of the absolute velocity C_u due to friction is

$$dC_u = \frac{\lambda}{4b} C_u C dt \quad (33)$$

The radial component of the absolute velocity C_m is the derivative of the distance R with respect to time t :

$$C_m = \frac{dR}{dt} \quad dt = \frac{dR}{C_m} \quad (34)$$

Substituting in equation (33) the above found value of dt we obtain finally the loss in the tangential component of the absolute velocity due to friction at the surface of the diffuser over a distance ds :

$$(dC_u)_{\text{fr}} = \frac{\lambda}{4b} C_u C \frac{dR}{C_m} = \frac{\lambda}{4b} \frac{C}{C_m} C_u dR = \frac{\lambda}{4b} \frac{dR}{\sin \alpha} C_u \quad (35)$$

On the other hand, if the frictional losses in the diffuser were not taken into consideration, the moment of momentum should remain the same, that is, $R C_u = \text{constant}$. Hence the tangential component of the absolute velocity in the motion of the fluid in the diffuser over path ds

should vary also with change in radius. This change can be obtained by differentiating the equation $R C_u = \text{constant}$:

$$C_u dR + (dC_u)_R R = 0$$

$$(dC_u)_R = - \frac{C_u dR}{R} \quad (36)$$

The total change in velocity during the displacement of the fluid in the tangential direction over the path ds is expressed as the sum of its changes due to the friction of the moving fluid at the diffuser walls $(dC_u)_{fr}$ and due to the continuous change in the radius $(dC_u)_R$, that is,

$$dC_u = (dC_u)_{fr} + (dC_u)_R = \frac{\lambda}{4b} \frac{dR}{\sin \alpha} C_u - C_u \frac{dR}{R} \quad (37)$$

Multiplying both sides of the above equation by R , we obtain

$$R dC_u + C_u dR = \frac{\lambda}{4b} \frac{dR}{\sin \alpha} RC_u$$

or

$$\frac{d(RC_u)}{RC_u} = \frac{\lambda}{4b} \frac{dR}{\sin \alpha} \quad (38)$$

The expression obtained can be simplified bearing in mind that

$$RC_u = R \frac{C_m}{\tan \alpha} = R \frac{Q_{sec}}{2\pi R b} \frac{1}{\tan \alpha} = \frac{Q_{sec}}{2\pi b \tan \alpha}$$

Then

$$d(RC_u) = \frac{Q_{sec}}{2\pi b} d(\cot \alpha)$$

Substituting in expression (38) $\tan \alpha / \sqrt{1 + \tan^2 \alpha}$ for $\sin \alpha$, we obtain the differential equation

$$\sec \alpha \, d \alpha = \frac{\lambda}{4b} \, dR \quad (39)$$

whose solution is

$$\log_e \frac{\sec \alpha + \tan \alpha}{\sec \alpha_3 + \tan \alpha_3} = \frac{\lambda}{4b} (R - R_3) \quad (40)$$

where

R_3 inlet radius to the diffuser

R variable radius varying from R_3 to R_a (diffuser outlet radius)

b width of diffuser

α_3 diffuser inlet angle

α angle formed by the true direction of the flow at radius R with the tangential component of the absolute velocity

λ coefficient of friction essentially a function of the roughness and varying, according to the results of numerous investigations conducted at the Blower Section on plywood diffusers, within the limits 0.05-0.15.

The entry angle of the flow into the diffuser α_3 has been determined above so that $\cos \alpha_3 / (1 + \sin \alpha_3)$ is a known value and for a given constant value of the coefficient λ we can, for given R_3 and R , transform expression (40) to the form

$$\frac{1 + \sin \alpha}{\cos \alpha} = K$$

Solving the above equation for $\sin \alpha$, we find the flow exit angle at radius R :

$$\sin \alpha = \frac{K^2 - 1}{K^2 + 1}$$

The radial component C_m at radius R can readily be determined from the continuity equation

$$C_m = \frac{Q_{sec}}{2\pi Rb}$$

while the tangential component will be equal to

$$C_u = \frac{C_m}{\tan \alpha}$$

Substituting the values of the exit velocity components C_m and C_u in equation (26) and $dR/\sin \alpha$ for ds , we obtain the general value of the losses due to friction in the diffuser:

$$\begin{aligned} dH_r &= \frac{\lambda}{4b} \rho \frac{C_m^2}{\sin \alpha} dR + \frac{\lambda}{4b} \rho \frac{C_u^2}{\sin \alpha} dR \\ &= \frac{\lambda}{4b} \rho \frac{C_m^2}{\sin \alpha} dR + \frac{\lambda}{4b} \rho \frac{C_m^2}{\sin \alpha \tan^2 \alpha} dR \\ &= \frac{\lambda}{4b} \rho \frac{C_m^2}{\sin \alpha} \left(1 + \frac{1}{\tan^2 \alpha} \right) dR \quad (41) \end{aligned}$$

Thus having explained the general scheme of the friction losses occurring in the diffuser, we proceed with the analysis of our test data. Our problem in analyzing these data reduces to the determination of the actual value of the friction coefficient (or more accurately, its mean value) for the air flow through the plane diffuser of our model blower. The procedure for determining this coefficient is analogous to the one applied in analyzing the performance of the impeller and reduces to a comparison of the experimental with the computed characteristics. Assuming various values of the coefficient λ , we obtain corresponding values of the friction losses through the diffuser, various values of the absolute velocity at the diffuser outlet, and hence various dynamic pressures at the diffuser outlet.

In the tables below are given the values characterizing the state of flow at the diffuser outlet for values of the friction coefficient $\lambda = 0.05, 0.1, \text{ and } 0.15$ and the values of the friction losses ΔH_{fr} determined by formula (41) (table 7).

The computed static head at the diffuser outlet can be obtained by subtracting from the total head at the diffuser inlet H_{dif} the impact head ΔH_{impact} the friction head ΔH_{fr} and the dynamic head at the diffuser outlet

$$\rho \frac{C_a^2}{2} :$$

$$H_{st \ dif} = H_{dif} - \Delta H_{impact} - \Delta H_{fr} - H_{dyn \ dif} \quad (42)$$

The obtained values of the static head are collected in table 8 and plotted in figures 20a and 20b.

As may be seen from the results obtained, the value of the coefficient λ for the plane diffuser of the first stage may be assumed equal to 0.1; for the diffuser of the second stage, a satisfactory agreement between the computed characteristic of the static head $H_{st \ comp}$ at the diffuser exit with the test characteristic $H_{st \ exp}$ is obtained for a value $\lambda = 0.15$ of the friction coefficient. The relatively large value of this coefficient obtained for the diffuser of the second stage may be explained by the considerably greater roughness of the wall surfaces for the diffuser of this stage.

We emphasize that the values found for the friction coefficient λ were obtained in investigating the flow through a diffuser constructed of plywood where the losses due to surface friction should be considerably greater than in the case of flow over a carefully treated metallic surface as such as often encountered in turboblowers. This circumstance should be borne in mind in designing vaneless diffusers and consideration given, each time in selecting the coefficient, to the material of which the diffuser is constructed and the care with which its surface has been treated. In projecting new turboblower designs the value of the coefficient λ for metallic surfaces may, for orientating purposes, be taken as approximately half the values of the coefficient obtained for plywood diffusers, that is, a value within the range 0.03-0.07 (Pfleiderer gives the coefficient within the same range).

4. Investigation of the Performance of the Reversing Guide Vanes

The last stage in our investigation of the model turboblower is the analysis of the losses occurring after exit from the diffuser. As may be seen from the sketch of the turboblower (fig. 3) at each stage of the model under consideration, these losses can be considered as made up of the following elementary components:

(a) Losses during the deflection of the flow in the meridional plane by 180° from the vaneless diffuser into the reversing guide vanes ΔH_1

(b) Losses during the flow through the reversing guide vanes ΔH_2

(c) Losses at the exit of the flow from the stage ΔH_3

The schematic division of the total losses into individual component parts and the neglecting of the mutual interference of the various factors is here particularly evident. As has been said above, however, we are constrained to make use of this approximation and consider each of these losses as independent of the others.

In correspondence to our general plan of the blower analysis, we obtain the total value of the losses $\Sigma\Delta H$ as the difference between the total head at the diffuser outlet H_{dif} and the total head at the stage outlet H_{stage} :

$$\Sigma\Delta H = H_{dif} - H_{stage} \quad (43)$$

The total head at the diffuser outlet H_{dif} entering the above equation is equal to the sum of the test values of the static head at the diffuser outlet $H_{st dif}$ and the velocity head of the absolute velocity at the diffuser outlet $H_{dyn dif}$, corresponding to the value of the friction coefficient λ assumed by us in the computation of the vaneless diffuser of each stage.

Similarly the total head at the stage outlet is equal to the sum of the test static head at the stage outlet H_{st} stage and the dynamic head H_{dyn} stage. The velocity at the stage outlet was determined from the continuity equation on the assumption of complete filling out of the outlet cross section.

Having thus determined the total value of the losses, we proceed to the consideration of the individual components.

a) Losses in deflection at the guide vanes.— The flow at the reversing guide vanes is deflected by 180° in a channel with expanding cross section after deflection. The investigation of the losses in channels of this shape has been described in a number of papers by Frey (reference 12), Nippert (reference 2), and others, the loss coefficients ξ_{defl} given by these authors differing somewhat. Thus, according to Frey, the value of the coefficient ξ_{defl} obtained by him in the investigation of a rectangular channel with increasing cross section provided with a deflector plate with the ratio of channel area after deflection to area before deflection $F_2/F_1 = 2$, fluctuates within the limits $\xi_{defl} = 2.5-3.0$. According to the tests of Nippert conducted on channels of considerably smooth shape and without a deflector plate $\xi_{defl} = 1.2-1.5$.

While the difference in the values of the coefficient ξ_{defl} can be explained by the fundamentally different construction of the elbows studied by these two authors the fact still remains that values of this coefficient are high and the losses involved in the deflection of a flow in a channel with expanding cross section are considerable. This phenomenon may be explained by the fact that in channels of such shape the turbulence formation usual in curved channels during deflection occurs with considerably greater intensity due to the separation of the flow from the deflector plate and the sudden decrease in the velocity at the entrance into the expanding parts of the channel. As a result there is a considerable increase in the vortex region and the general value of the losses in flowing through a channel of such shape increases.

The photographs taken from the work of Frey (fig. 21) and Bucowski (fig. 22) (reference 13) of the flow through a curved channel with expanding section clearly confirm the necessity for relatively high values of the loss coefficient ξ_{defl} in flowing through a channel of such shape.

In analyzing the test data the value of this coefficient for a deflection with the ratio $F_2/F_1 = 1.6$ was assumed to have the value 2. The value of the deflection losses ΔH_1 referred to the dynamic pressure of the radial component of the absolute velocity at the exit of the vaneless diffuser $\rho \frac{C_m^2}{2}$ is therefore given by the equation

$$\Delta H_1 = \xi_{\text{defl}} \rho \frac{C_m^2}{2} = 2.0 \rho \frac{C_m^2}{2} \quad (44)$$

b) Losses at entrance and during flow through the guide vanes. - Before proceeding to the consideration of the losses in the reversing guide vanes, it must be noted that the transformation of the velocity head at the impeller exit into static head is essentially completed before entrance into the reversing guide vanes. The absolute velocity of the flow at entrance and in flowing through the guide vanes is thus relatively small and therefore the losses in the guide vanes should constitute only a small part of the entire hydraulic losses of the blower. The losses in this element of the multistage blower consist, first of all, of the impact losses at the stationary blade in entering the guide vanes, and secondly of the losses associated with the change in the absolute velocity at the guide vanes from the value C_4 (inlet velocity to the guide vanes) to the value C_5 (outlet velocity from the guide vanes). The value of the absolute inlet velocity to the guide vanes was determined as follows: The value of its tangential component C_{4u} during the deflection by 180° remains naturally unchanged. Taking account of the contraction of the flow at the place of deflection (due to the separation from the wall) we consider the value of the radial component C_{4m} also to be equal to the value of this component at the diffuser outlet, that is, $C_{4m} = C_{3m}$. The absolute inlet velocity to the guide vanes can thus be determined from the expression

$$C_4 = \sqrt{C_{4m}^2 + C_{4u}^2} = C_3$$

For the flow between the guide vanes it may with sufficient

degree of accuracy be assumed that the flow rotation characterized by the tangential component of the absolute velocity C_u ceases and the flow at the guide vanes exit flows in a purely radial direction. The value of the absolute velocity at the guide vanes exit is thus determined directly from the equation of continuity.

The impact loss at the entrance to the stationary vanes is conveniently referred to the dynamic pressure of the absolute inlet velocity C_4 and expressed in the form $\xi \rho \frac{C_4^2}{2}$ where ξ is a coefficient that takes ac-

count of the part of the kinetic energy lost at the guide vanes inlet. The value of this coefficient, according to investigations conducted on guide vanes in elbows (reference 14) by the Blower Section of CAHI was taken as constant for both stages and equal to the value 0.3.

In order to find whether the inlet angle to the guide vanes affects this group of losses the vanes in the tested model were curved backward permitting a deflection about the axis of $\pm 10^\circ$. The large number of characteristics obtained for various positions of the vanes showed that the change in the angle of attack within relatively wide limits has almost no effect on the characteristics of the individual stages and of the blower as a whole. At least within the limits of the experimental accuracy no changes in the test characteristics could be observed. This may be explained by the fact that, on the one hand, as is seen from the sketch of the blower (fig. 3) the blades were so well rounded and streamlined that the entry shock at the stationary vane, even for large angles of attack, was reduced as a result of the smoothness of the vane shape. On the other hand, the absolute velocity at the inlet to the guide vanes was very small so that a change in the angle of attack within relatively wide limits and a corresponding change in the value of the coefficient ξ only very slightly changed the absolute value of the impact losses at the guide vanes inlet so that this change had no effect on the characteristic curves obtained.

The losses associated with the velocity decrease in the reversing guide vanes were computed by the usual formula giving the impact loss:

$$\Delta H_{\text{impact}} = \frac{(C_4 - C_5)^2}{2} \rho \quad (45)$$

Finally the last group of losses is associated with the jet contraction at the stage outlet and was computed by the formula

$$\Delta H_{\text{exit}} = \xi_{\text{exit}} \rho \frac{C_{\text{exit}}^2}{2} \quad (46)$$

The value of the coefficient ξ_{exit} for both stages was taken equal to 0.4.

The computed value of the total head at the stage outlet H_{stage} was then determined as the difference between the value of the total head at the diffuser outlet H_{dif} and the sum of all the computed losses from the diffuser outlet to the stage outlet $\Sigma\Delta H$.

To obtain the static head at the stage outlet it is necessary to subtract from the obtained value of the total head H_{stage} the dynamic head at the stage outlet

$H_{\text{dyn exit}}$:

$$H_{\text{st stage}} = H_{\text{dif}} - \Sigma\Delta H - H_{\text{dyn exit}} \quad (47)$$

The results obtained are given in table 9. Figure 23 gives a comparison of the computed characteristics of the static heads at the stage outlet with the characteristics obtained experimentally.

III. CONCLUSIONS

1. The method applied for the investigation of the multistage centrifugal blower of successive consideration of the performance of its individual elements (impeller, vaneless diffuser, etc.), notwithstanding a certain degree of approximation involved, clearly brings out the magnitude and character of the losses that occur in the flow through the centrifugal blower and also the physical meaning and values of the coefficients that characterize these losses.

2. Due to the fact that the investigation of the blower performance was conducted for various air volumes delivered, it was possible to obtain the dependence of the individual loss coefficients on a number of factors (the angle of blade attack, the velocity of approach, etc.).

3. The investigation of the performance of the vaneless diffuser behind the impeller permitted determination of the character of the losses that arise in the transformation of the velocity head at the impeller outlet into static head and to determine the limits within which the friction coefficient λ varies in the flow through the vaneless diffuser.

4. With the aid of coefficients having a sufficiently well defined physical meaning, it was possible to compute the centrifugal blower on the basis of a more or less schematic consideration of the flow phenomena that occur without having recourse to similarity computations and avoiding the introduction of arbitrary correction coefficients.

5. Finally it should be noted that it was not possible naturally in this paper to exhaust the large number of problems associated with the investigation of multi-stage centrifugal machines, the present investigation constituting only one of a series of investigations by the Blower Section devoted to the study of the working process in such machines. The investigations at present being conducted on guide vanes, spiral casings, labyrinth packings, and so forth, may throw light on a whole series of problems of extreme importance in the computation and design of high-pressure centrifugal blowers.

APPENDIX

ON THE APPLICATION OF RESULTS OBTAINED FROM
MODEL TESTS TO FULL-SCALE DESIGN

The testing of large turbomachines is a very costly and laborious procedure and at the same time practically affords no possibility of making a satisfactory analysis of their performance because such kind of investigation generally is of the nature of a routine or acceptance test. The explanation for this lies chiefly in the complexity in the preparation of large machines for scientific investigations and in the practical impossibility of connecting large machines to accurate dynamometers.

There are still a number of other reasons that render difficult the investigation of the performance of full-scale large machines. Considerations of strength, for example, at times do not permit the introduction of desired modifications of the impellers for purposes of investigation. Purely mounting considerations often do not permit in large machines making modifications and changes such as would present no difficulty in the testing of specially designed models. Such, for example, are the tests of the impeller alone, impeller with diffuser and without guide vanes, the introduction of various modifications in the shape of the spiral casing, etc.

In testing with a motor intended for normal utilization and the power of which is specially chosen for this purpose, it is necessary to test the blower over a relatively narrow range of operating conditions and avoid inadmissible overloading of the motor.

The above considerations make it preferable in many cases to test geometrically similar models rather than the full-scale machine itself. Similarly in the design of new machines it is much more convenient in many cases to conduct preliminary tests on one or several relatively inexpensive models before proceeding to the entire expensive setup which moreover lends itself with difficulty to modifications.

To a first rough approximation the transition from the results of model tests to full-scale may be effected with the aid of the elementary relations of geometric

similitude. If the values referring to the model are denoted by the subscript M and those referring to the full-scale machine are without subscript, these relations may be formulated as follows. If the respective fluid (gas) volumes satisfy the relation

$$\frac{Q_M}{Q} = \frac{n_M D_M^3}{n D^3} \quad (48)$$

then the following equality determined by the similarity of the kinetics of the two flows is satisfied

$$\eta_M = \eta_{f.s.} \quad (49)$$

The above equation is true for all efficiencies of the machine, the over-all static coefficient of friction, the hydraulic efficiency, the adiabatic efficiency, etc. This equation corresponds to the equality of all the coefficients of the losses within the machine, the exponents of the polytropic pressure curves, and to the machine as a whole as well as to its parts.

$$\frac{H_M}{H} = \frac{\gamma_M n_M^2 D_M^2}{\gamma n^2 D^2} \quad (50)$$

The above equation also holds for all pressures under consideration: the total, static, and dynamic pressures.

For the power required we have the equation

$$\frac{N_M}{N} = \frac{\gamma_M n_M^3 D_M^5}{\gamma n^3 D^5} \quad (51)$$

where, in analogy to what was said above, the power N may be considered as the total required power (with the exception, of course, of the mechanical losses) as well as the partial power expenditures in the air friction of the disks and the losses through the clearances.

The above equations (48) to (51) give satisfactory results for those cases where the difference in the dimensions and the rotational speeds of model and full-scale

lies within relatively narrow limits. In order to solve the problem of what these limits are for which the application of the elementary similitude formulas are applicable, we shall consider what further criterions must be introduced to supplement the geometric and kinematic conditions taken into account by formulas (48) to (51).

Such criterions are two in number, namely the Reynolds and the Bairstow* numbers which we shall now consider in turn.

The similitude criterion of Reynolds, that is, the requirement that the Reynolds number

$$Re = \frac{cd}{\nu}$$

for full-scale and model should be equal, corresponds to the requirement of maintaining dynamic similitude between the inertia forces (mass forces) and the frictional forces (surface forces) that are characterized by the viscosity. Since the testing of model blowers is conducted in air, the same gas with which the full-scale blower is to operate, the condition

$$Re_M = Re \quad \frac{C_M d_M}{\nu_M} = \frac{Cd}{\nu}$$

leads to the equation

$$C_M d_M = Cd$$

In maintaining dynamic similitude the velocities at any point of the machine are proportional to the product nD and any characteristic dimension d is proportional to the diameter. From the equality of the Reynolds numbers for model and full-scale we have the equation

$$n_M D_M^2 = n D^2 **$$

*More commonly denoted as the Mach number. Trans.

**Where $\nu_M \neq \nu$ we have the equation

$$\frac{m_M D_M^2}{\nu_M} = \frac{n D^2}{\nu}$$

or

$$U_M D_M = U D \quad \frac{U_M}{U} = \frac{D}{D_M}$$

Since the material of the rotor of the full-scale machine works under stresses that are near the maximum admissible the satisfying of the last condition for a model scale that is very different from unity is not possible. The dynamic similitude of the phenomena is then disturbed and equations (48) to (51), strictly speaking, cease to be valid. In passing from model to full-scale it is necessary to introduce computational corrections on the magnitude of the pressures and powers (equations (49) to (51)). The first condition, namely, that of dynamic similitude, evidently remains unchanged.

In correcting for the scale of dimensions of model and full-scale the most extensive data have been gathered in the field of hydraulic turbines where the formula of Moody is used:

$$\eta = 1 - \left[(1 - \eta_M) \left(\frac{D_M}{D} \right)^{\frac{1}{4}} \left(\frac{H_M}{H} \right)^{\frac{1}{10}} \right]$$

The expression within the bracket and equal to $(1 - \eta)$ evidently characterizes the magnitude of the hydraulic losses in the turbine. Taking account of the known degree of approximation of this formula, it is entirely permissible to substitute in it for the ratio H_M/H the ratio

$\frac{\eta_M D_M^3}{\eta D^3}$ (see equation (50)) and for the exponent $1/10$ to

substitute $1/8$. Even for ratios H_M/H of the order of $1/10$ such substitution leads to an error of the order of 2 to 3 percent which certainly lies within the limits of experimental error particularly since geometrical similitude cannot be accurately maintained.

Making the above substitutions in the equation of Moody we obtain the equation

$$\eta = 1 - \left[(1 - \eta_M) \left(\frac{\eta_M^2 D_M^4}{\eta^2 D^4} \right)^{\frac{1}{8}} \right]$$

or

$$\eta = 1 - \left[(1 - \eta_M) \left(\frac{Re_M}{Re} \right)^{\frac{1}{4}} \right]$$

The above equation states that the losses in the turbine are inversely proportional to the fourth power of the Reynolds number.

Notwithstanding the fact that in the hydraulic turbine, in contrast to the pump or blower, the main losses are the friction losses, the above conclusion should not be considered as a generalization to some extent of the analogous formula of Blasius for the friction loss coefficient in smooth pipes:

$$\lambda = \frac{0.3164}{Re^{0.25}}$$

The Blasius formula, as is shown by experiment, is applicable only to those cases where the corresponding Reynolds number, determining also the turbulence of the flow, lies within the limits 10,000-15,000. In large machines the turbulence of the flow is certainly considerably greater and the Reynolds numbers defined for the hydraulic diameters of the main passages are much higher. For this reason, the apparent agreement of the Moody and the Blasius formulas must be considered as accidental. In general, the decrease in the friction losses in smooth channels at large Reynolds numbers should be at a considerably slower rate than corresponds to the exponent 1/4. The considerable decrease in the losses on increasing the dimensions corresponding to the formula of Moody should therefore be considered as due not to the change in the dynamic flow conditions themselves but rather first to the change in the relative roughness of the surfaces, and second to the impossibility of maintaining similitude of full-scale and model in the details (rivets, nuts, soldered joints, etc.).

The application of the results of a number of tests on models of centrifugal machines to full-scale and comparison with the results of full-scale tests has shown that the formula of Moody gives values that are too large. The reason for the unsuitability of the formula of Moody in this case is to be ascribed essentially to the fact that, in contrast to hydraulic turbines, centrifugal compressors constitute a system of diffusers in which the

resistances are more in the nature of local than linear (frictional) resistances. Since these local resistances, to a much less degree than the linear resistances, depend on the Reynolds number and on the surface roughness the difference between full-scale and model for centrifugal compressors should be considerably less than for hydraulic turbines.

On the basis of the above considerations, that is, assuming the correctness of the Moody law for the friction losses and assuming the coefficient of the local losses as constant, we obtain the following method of computing the full-scale blower from the model tests as applied in the Blower Section of CAHI.

The main assumption underlying this method is that all linear losses occurring in the blower (friction in the vaneless diffuser, air friction of the disk, etc.) are computed by the elementary similitude formulas taking account of the difference in the full-scale and model Reynolds numbers (Moody formula). The local resistances, however, (the losses in the impeller, guide vanes, etc.) are computed only by the similitude formulas, the coefficients of local resistance obtained in investigating the results of model tests being assumed constant both for the model and full-scale blower. The computational procedure is as follows. Having computed the full-scale required power from the model power, we divide the power into two parts (fig. 24), namely, N_{hM} the hydraulic power of the model determined by the kinematics of the flow and computed by the elementary similitude formulas

$$N_h = N_{hM} \frac{n^3}{n_M^3} \frac{D^5}{D_M^5}$$

and the power required to cover the blower losses and expended essentially in air friction of the impeller disks and which is computed by the similitude formula with account taken of the Reynolds number

$$N_O = N_{OM} \frac{n^3}{n_M^3} \frac{D^5}{D_M^5} \left(\frac{Re_M}{Re} \right)^{\frac{1}{4}}$$

The pressure head for the full-scale blower is computed in the following manner. The magnitude of the

theoretical head H_{th} developed for a given air volume Q and given hydraulic power N_h is

$$H_{th} = \frac{75 N_h}{Q_{sec}}$$

The pressure losses

$$\Delta H = H_{th} - H_{exp}$$

are divided into two parts, namely, the losses due to friction (losses in the vaneless diffuser, casing) and losses due to the local resistances (losses in the impeller, impact losses in the casing, etc.).

$$\Delta H = \Delta H_{lin} + \Delta H_{local}$$

The pressure losses obtained on the model are computed for the full-scale as follows:

$$\Delta H_{lin} = (\Delta H_{lin})_M \frac{n^2 D^2}{n_M^2 D_M^2} \left(\frac{Re_M}{Re} \right)^{\frac{1}{4}}$$

$$\Delta H_{local} = (\Delta H_{local})_M \frac{n^2 D^2}{n_M^2 D_M^2}$$

The pressure developed by the full-scale blower is determined from the relations

$$H_{th} = H_{th M} \frac{n^2 D^2}{n_M^2 D_M^2}$$

$$\Delta H = \Delta H_{lin} + \Delta H_{local}$$

$$H = H_{th} - \Delta H$$

Having the pressures H_M and powers N_M for various values of Q_M - we thus obtain a series of values of Q , H , and N after which the determination of the efficiency and the construction of the characteristics for the full-scale blower offer no difficulties.

The chief difficulty in the above explained method of computation for full-scale lies in the fact that this method assumes available both experimental and computed model characteristics that agree with each other. Only in such case is a distribution of the losses possible, a procedure that is fundamental for the entire method.

The present paper represents a typical model investigation having for its object the obtaining of a clear picture of the distribution of the losses. From this point of view it is one of a series of investigations conducted at CAHI on models of industrial and experimental types. This kind of combined experimental and computational work on models is therefore conducted under such conditions that full-scale computation becomes possible only on obtaining satisfactory agreement between the computed and test curves. This rather strict requirement, which is a source of considerable difficulties, at the same time leads to the accumulation of extremely valuable data both from the point of view of the subsequent computations and for the analysis of the performance of centrifugal blowers.

It should be noted that although the above computation method gave satisfactory results even in some cases for a ratio of 10 of full-scale and model Reynolds numbers, it cannot be said that this confirms its complete reliability. The method is still a "young" one and the correctness of any method for computing full-scale data from the model can be proved only statistically.

In any case the above described method of investigation makes it possible to judge clearly the performance of a model and apply the results to full-scale. It should nevertheless be noted that the transition to full-scale by the elementary similitude formulas gives lowered values for the pressure and exaggerated values for the power and, finally, decreased values of the efficiency for the full-scale machine. The computation by the Moody formula gives

exaggerated values of the efficiency.* The method of breaking up the losses into component parts which gives mean values of the efficiency has every reason for giving the best agreement of the computational with test results.

The above described method of computing the full-scale characteristics from the tests on the model gives an exhaustive solution only for the case where the centrifugal machines under investigation operate with an incompressible fluid having a constant density. Such machines, for example, may be pumps or blowers developing pressures of the order of 100 to 200 millimeters water. Practically, even for higher pressures of the order of 1000 to 1500 millimeters water the computation by the above method may be admissible, a mean density being used.

In those cases, however, where the ratio of the outlet pressure P_2 to the inlet pressure P_1 (compression ratio) is greater than 1.1-1.2, it is necessary to consider the compressibility of the gas and take into account its change of density in compression. In that case the single equation (52)

$$\frac{Q_M}{Q} = \frac{n_M D_M^3}{n D^3}$$

is not sufficient for satisfying the kinematic similitude of the flow through the machine. This condition only assures similarity of the velocity diagrams at the impeller inlet. In the case of an incompressible fluid this condition also assures similarity of the velocity diagrams at the impeller outlet and kinematic similitude of the entire flow through the casing. Since in the flow of a compressible fluid there is a continuous change in volume, it is evident that kinematic similitude can be maintained only in the case where the changes in the volume of the gas are similar. In other words, if the ratio of the

* For the ratio $\frac{Re}{Re_M} \leq 2$ the taking account of the effect of the Reynolds number in computing full-scale data from the model tests is irrational since the correction obtained lies within the limits of accuracy of the computation. For $\frac{Re}{Re_M} > 4$ the corrections attain values of the order of 10 percent, i.e., become essentially necessary.

volume of the gas flowing through any cross section of the model to the volume of the inducted gas is equal to the corresponding ratio for full-scale: *

$$\left(\frac{v_2}{v_1}\right)_M = \frac{v_2}{v_1}$$

If all the remaining conditions of complete similitude are simultaneously satisfied, that is, there is complete geometric similitude between model and full-scale, the condition of kinematic similitude of the velocity diagrams at the inlet is satisfied (equation (52)); the Reynolds numbers of full-scale and model are equal and the requirement of similar change in the volumes is equivalent to satisfying the equality of the Bairstow numbers for full-scale and model. This can be shown with the aid of the following sufficiently elementary considerations:

The unit work in kilogram-meters per kilogram required by the blower (full-scale) is

$$H = \frac{\phi_2 U_2^2}{g} = \frac{k}{k-1} RT_1 \left[\left(\frac{v_1}{v_2}\right)^{m-1} - 1 \right] \frac{\text{kg-m}}{\text{kg}} \quad (52)$$

Correspondingly the work per kilogram gas required by the model is

$$H_M = \frac{\phi_{2M} U_{2M}^2}{g} = \frac{k}{k-1} RT_{1M} \left[\left(\frac{v_1}{v_2}\right)_M^{mM-1} - 1 \right] \frac{\text{kg-m}}{\text{kg}} \quad (53)$$

Taking their ratio we obtain

$$\frac{H_M}{H} = \frac{\phi_{2M} U_{2M}^2}{\phi_2 U_2^2} = \frac{RT_{1M} \left[\left(\frac{v_1}{v_2}\right)_M^{mM-1} - 1 \right]}{RT_1 \left[\left(\frac{v_1}{v_2}\right)^{m-1} - 1 \right]} \quad (54)$$

It was assumed above equality of the adiabatic efficiencies and of the exponents of the compression polytropics as a

*The process here considered is that occurring in uncooled turboblowers in which the change in volume is due entirely to internal processes in the machine.

consequence of complete kinematic similitude between full-scale and model. Moreover, the kinematic similitude implied also equality of the deflection coefficients φ_2 for full-scale and model.

Dividing out equal factors in equation (54) we obtain finally that for similar volume change v_1/v_2 for full-scale and model we have

$$\frac{H_M}{H} = \frac{U_{2M}^2}{U_2^2} = \frac{RT_M}{RT} \quad (55)$$

But

$$C_{\text{sound}} = \sqrt{k \frac{P}{\rho}} = \sqrt{kRT}$$

Hence the condition of similar volume changes may be written

$$\frac{U_{2M}^2}{U_2^2} = \frac{RT_M}{RT} = \frac{C_{\text{sound } M}^2}{C_{\text{sound}}^2} \quad (56)$$

In the majority of cases the model tests are conducted with air of about the same temperature as the intake air under the operating conditions of the blower itself.* This means that satisfying the equality of the Bairstow numbers requires the equality of the peripheral speeds

$$U_{2M} = U_2$$

or

$$n_M D_M = nD$$

This condition can be satisfied only in exceptional cases since the impellers of centrifugal compressors working at relatively high degree of compression usually have relatively high peripheral speeds. To maintain the same speed for models makes great demands on the model as

* An exception is formed by the centrifugal superchargers of aviation engines for which the operating temperatures may sharply differ from those under the model test conditions.

regards strength requirements and for large scale ratio, may lead to speeds of the model that are technologically difficult to attain. For this reason the equality of the Bairstow numbers in the large majority of cases is incapable of being satisfied and in those cases kinematic similarity under conditions of compressibility of the gas is, strictly speaking, impossible. It is therefore only possible to speak of a more or less approximate method of passing from the model to full-scale that would satisfy practical requirements.

The experience gained in tests on a number of blowers of computing from one speed to other speeds and the work of foreign investigators (reference 15) makes it possible to state that even for ratios of Bairstow numbers for full-scale and model of 1.5:2 the elementary formulas of similitude may be applied with a sufficient degree of accuracy. The relations between the various magnitudes obtained in testing the model and the full-scale machine as formulated above should, taking account of the thermodynamic aspect of the phenomena, be transformed as follows.

If the volumes of the gas inducted by the model and full-scale satisfy the relation

$$\frac{Q_M}{Q} = \frac{n_M D_M^3}{n D^3}$$

then, neglecting the difference in the kinematics of the two flows due to different change in the unit volumes in full-scale and model it may, to a first approximation, be assumed that the exponent of the compression polytropic, the adiabatic and hydraulic efficiencies remain the same. Then:

1. The work per kilogram of gas required by model and full-scale will be in the ratio of the squares of the peripheral speeds

$$\frac{H_M}{H} = \frac{U_{2M}^2}{U_2^2} = \frac{n_M^2 D_M^2}{n^2 D^2} \quad (57)$$

Between the unit work H and the compression ratio P_2/P_1 of the tested compressor the following relation can be set up

$$\begin{aligned}
 H &= \frac{C_{2u}U_2}{g} = \frac{C_p}{A} (T_2 - T_1) = \frac{C_p}{A} T_1 \left[\left(\frac{T_2}{T_1} \right) - 1 \right] \\
 &= \frac{C_p}{A} T_1 \left[\left(\frac{P_2}{P_1} \right)^{\frac{m-1}{m}} - 1 \right] = \frac{k}{k-1} RT_1 \left[\left(\frac{P_2}{P_1} \right)^{\frac{m-1}{m}} - 1 \right] \frac{\text{kg-m}}{\text{kg}} \quad (58)
 \end{aligned}$$

$$\left(\frac{P_2}{P_1} \right)^{\frac{m-1}{m}} = \frac{C_{2u}U_2A}{gC_pT_1} + 1$$

Hence

$$\frac{P_2}{P_1} = \left[\frac{C_{2u}U_2A}{gC_pT_1} + 1 \right]^{\frac{m}{m-1}} \quad (59)$$

2. The rise in temperature of the compressor Δt is proportional to the square of the peripheral speed. Thus

$$\frac{T_2}{T_1} = \left(\frac{P_2}{P_1} \right)^{\frac{m-1}{m}}$$

$$\frac{T_2 - T_1}{T_1} = \frac{P_2^{\frac{m-1}{m}} - P_1^{\frac{m-1}{m}}}{P_1^{\frac{m-1}{m}}}$$

$$\frac{\Delta t'}{\Delta t} = \frac{P_2'^{\frac{m-1}{m}} - P_1^{\frac{m-1}{m}}}{P_2^{\frac{m-1}{m}} - P_1^{\frac{m-1}{m}}} = \frac{\left(\frac{P_2'}{P_1} \right)^{\frac{m-1}{m}} - 1}{\left(\frac{P_2}{P_1} \right)^{\frac{m-1}{m}} - 1} = \frac{H'M}{H} = \frac{U_2M^2}{U_2^2} \quad (60)$$

3. The power required by the compressor (except for the mechanical losses) varies as the cube of the peripheral speed

$$\frac{N_M}{N} = \left(\frac{U_{2M}}{U_2} \right)^3 \quad (61)$$

This follows immediately from the condition of kinematic similitude.

The admissibility of passing from the results of model tests to full-scale or computing the results of tests on centrifugal compressors from one speed to another, making use of the above relations, may be shown by the centrifugal supercharger test characteristics computed from the results of Brooke (reference 16) (figs. 25a, b, c, and d).

Comparison of the test characteristics of the supercharger, obtained for $n = 20,000$ rpm, with the characteristics obtained by the use of the elementary formulas for computing the characteristics at 20,000 rpm from the test characteristics at 14,000 rpm shows a deviation between the computed and test characteristics not exceeding the ordinary experimental accuracy.

It is evident that the error obtained with this method of computation is considerably greater if we are considering not a single stage centrifugal compressor but a multistage blower. In this case the deviation of the flow kinematics due to the continuous change in the density of the gas is successively added up along the path through the machine thereby considerably changing the total value of the losses. Nevertheless, notwithstanding its large approximation this method, for cases where the Bairstow numbers for full-scale and model differ slightly, gives satisfactory agreement for practical computations.*

In those cases, however, where the Bairstow numbers for full-scale and model differ considerably, the computation by the above elementary similitude formulas may lead to very large error and disagreement between the computed and test characteristics. In this case the only method of computation that gives results with any degree of accuracy is the above method of successive analysis of the elements of the machine and which is a combination of experimental investigation with technical computation.

*The effect of the ratio of the Bairstow numbers plays an essential part only for absolute values of the larger of the two Bairstow numbers within the limits 0.4-0.7; for smaller values the effect of the compressibility of the gas is negligible; for larger values, in connection with the approach to the velocity of sound, all computations become subject to doubt.

The first stage of the computation, in correspondence to the procedure described above, is the construction of the computed model characteristics giving satisfactory agreement with the results of experimental investigation both for the entire model and for its individual elements. From this stage of the investigation the kinematics of the flow is clarified and the values of the coefficients of the local resistances of the machine obtained. In the further computation the flow phenomena and the coefficients are considered the same both for model and full-scale.

The next step is the transition from the obtained curves of the model to full-scale with account taken of the change in the friction losses in correspondence with the law of Moody and of the continuous change of the density of the flow through the machine.

Such computation of the machine according to its elements can be conducted either analytically or (preferably) graphically with the aid of entropy diagrams (I-S, T-S). It should be emphasized that such computations are reliable only in the case where the Bairstow number for the full-scale machine has a value sufficiently different from unity. This is explained in the first place by the fact that on approaching the velocity of sound the character of the resistance itself undergoes change. The law of linear resistance, for example, rapidly begins to deviate from the square law and approaches the cubic law. For velocities equal and above the velocity of sound wave resistance, pressure shocks, etc., make their appearance.

Since, under the flow conditions in the blower passages, there are a large number of guide surfaces and sections giving rise to vorticity, the local velocities may be considerably greater than the mean velocities. For this reason the above mentioned phenomena may occur even in the case where for the mean velocities of flow the Bairstow number is still far below unity.

Practically the use of the above computation methods for passing from model to full-scale may be considered admissible up to values of the peripheral speed of the impeller of the order of 240 to 250 meters per second which corresponds to a value of about 0.7 of the Bairstow number. We may note that also in the ballistic computations in deriving the formulas of Siacci (reference 17) the square law of the dependence of the resistance on the velocity is applied up to the velocities of the order of

240 meters per second. Since the above limiting velocities lie somewhat higher than those usually applied in turbomachines, the above described method of computation may have wide application in the design and testing of most machines.

As regards superchargers and blowers operating with peripheral speeds of the order of 300 to 400 meters per second, their investigation should be conducted at supersonic speeds near those of the full-scale machine. The study of the performance of such machines on models working with small peripheral speeds is admissible only for the purpose of obtaining a very rough first approximation. Every generalization of the data obtained to full-scale requires careful study of all thermodynamic factors entering the computation and strict taking account of all specific features of performance at supersonic speeds.

Translation by S. Reiss,
National Advisory Committee
for Aeronautics.

REFERENCES

1. Thoma, D., and Fischer, K.: Investigation of the Flow Conditions in a Centrifugal Pump. Trans. A.S.M.E., Nov. 1932.

Hagmayer, E.: Messungen des Druckverlaufes über Lauf- und Leitschaufel einer Kreiselpumpe innerhalb und ausserhalb des Gebietes der Kavitation. (Dissertation) Braunschweig, 1932.
2. Nippert, H.: Über den Strömungsverlust in gekrümmten Kanälen. Forschungsarbeiten auf dem Gebiete des Ingenieurwesens. Heft 320.

Bambach, R.: Plötzliche Umlenkung vom Wasser in geschlossenen unter Druck durchströmten Kanälen. Forschungsarbeiten auf dem Gebiete des Ingenieurwesens. Heft 327.

Nikuradse, Johanna: Untersuchungen über die Strömungen des Wassers in konvergenten und divergenten Kanälen. Forschungsarbeiten auf dem Gebiete des Ingenieurwesens. Heft 289, 1929.
3. Kirchbach: Der Energieverlust in Kniestücken. Mitteilungen des Hydraulischen Instituts der Technischen Hochschule. (Munich) 1929.

Schubart: Der Energieverlust in Kniestücken bei glatter und raucher Wandung. Mitteilungen des Hydraulischen Instituts der Technischen Hochschule (Munich) 1929.
4. Pfleiderer, C.: Die Kreiselpumpen. Berlin, 1924.

Stodola, Aurel: Die Dampf- und Gasturbinen. Berlin, 1924.

Kissina L., and Chebisheva, K.: Determination of the Power Expended in Rotating Disks in a Flow. CAHI, No. 211, 1935. (Russian)
5. Polikovskiy, V. I.: On the Computation of Centrifugal Blowers and Pumps. Pt. I. GTTI, 1934.

6. Polikovsky, V. I., and Gembarzhevsky, M.: Determination of the Contraction Coefficient of a Jet in Deflection. CAHI, No. 211, 1935. (Russian)
7. Polikovsky, V. I., and Nevelson, M.; On the Computation of Centrifugal-Blower Impellers. Pt. II.
8. Polikovsky, V. I.: On the Computation of Centrifugal Blowers and Pumps. Part II. GTTI, 1934.
9. Gibson: Hydraulics and Its Applications. GTTI, 1934.
10. Karrard, A.: Sur le calcul des roues centrifuges. La technique moderne. 1923.
11. Polikovsky, V. I., and Nevelson, M.; The Performance of Vaneless Diffuser Fan. T.M. No. 1038, NACA, 1942.
12. Frey, Kurt: Verminderung des Strömungsverlustes in Kanälen durch Leitflächen. Forschung auf dem Gebiete des Ingenieurwesens, no. 5, May-June 1934, pp. 105-117.
13. Bucowski: Technica laboratoryjna pomiarow aerodynamicznych. Warsaw, 1933.
14. Baulin, K., and Idelchik, I.: Experimental Investigation of the Motion of Air Through Elbows. M. Gosmashmetizdat, 1934.
15. Capon, R. S., and Brooke, G. V.: The Application of Dimensional Relationships to Air Compressors, with Special Reference to the Variation of Performance with Inlet Conditions. R. & M. No. 1336, British A.R.C., 1930.
16. Brooke, G. V.; Surging in Centrifugal Superchargers. R. & M. No. 1503, British A.R.C., 1933.
17. Loitsansky, L. T., and Lurye, A. I.: Theoretical Mechanics, vol. II. GTTI, 1933, pp. 51-54.

TABLE 1
THEORETICAL (TOTAL) PRESSURE AT IMPELLER OUTLET
DETERMINED FROM THE HYDRAULIC POWER N_h

| a) First Stage Impeller | | | | | |
|-------------------------|-----------|----------------------|-------|----------|----------|
| Q_{hr} | Q_{sec} | $H_{st \text{ exp}}$ | N_h | C_{2u} | H_{th} |
| 600 | 0.167 | 76.0 | 0.31 | 27.2 | 139.0 |
| 1000 | .278 | 74.0 | .49 | 25.8 | 132.0 |
| 1400 | .390 | 69.0 | .64 | 24.1 | 123.0 |
| 2000 | .555 | 53.0 | .77 | 20.4 | 104.0 |
| 2500 | .695 | 30.0 | .81 | 17.1 | 87.0 |

| b) Second Stage Impeller | | | | | |
|--------------------------|-----------|----------------------|-------|----------|----------|
| Q_{hr} | Q_{sec} | $H_{st \text{ exp}}$ | N_h | C_{2u} | H_{th} |
| 600 | 0.167 | 72.0 | 0.32 | 28.1 | 143.0 |
| 1000 | .278 | 69.0 | .51 | 26.9 | 137.5 |
| 1400 | .390 | 64.0 | .66 | 24.8 | 127.0 |
| 2000 | .555 | 55.0 | .79 | 20.9 | 106.5 |
| 2500 | .695 | 37.0 | .81 | 17.1 | 87.0 |

TABLE 2
FLOW AT INLET TO IMPELLER

| a) First Stage Impeller $\beta_1 = 148^\circ$, $U_1 = 24.6 \text{ m/sec}$, $\varphi_1 = 0.35$, $\mu = 0.9$ | | | | | | | |
|------------------------------------------------------------------------------------------------------------------|----------|---------------------------------------------------|-----------------------|------------|----------------|-----------------|-----------------|
| Q_{hr} | C_{1m} | $W_1 = \sqrt{C_{1m}^2 + (1 - \varphi_1)^2 U_1^2}$ | $W_1 = \frac{Q}{F_1}$ | W_{1max} | $\sin \beta_1$ | β_{1fl} | α |
| 600 | 6.12 | 17.1 | 13.7 | 17.1 | 0.358 | 159° | 11° |
| 1000 | 10.2 | 19.0 | 22.8 | 22.8 | .537 | $147^\circ 30'$ | $-30'$ |
| 1400 | 14.3 | 21.5 | 32.0 | 32.0 | .660 | $188^\circ 10'$ | $-9^\circ 50'$ |
| 2000 | 20.4 | 25.9 | 45.5 | 45.5 | .789 | 128° | -20° |
| 2500 | 25.5 | 30.0 | 57.0 | 57.0 | .85 | $121^\circ 40'$ | $-26^\circ 20'$ |

| b) Second Stage Impeller $\beta_1 = 143^\circ 50'$, $U_1 = 28.8 \text{ m/sec}$, $\varphi_1 = 0.4$, $\mu = 0.98$ | | | | | | | |
|-----------------------------------------------------------------------------------------------------------------------|----------|---------------------------------------------------|-----------------------|------------|----------------|-----------------|-----------------|
| Q_{hr} | C_{1m} | $W_1 = \sqrt{C_{1m}^2 + (1 - \varphi_1)^2 U_1^2}$ | $W_1 = \frac{Q}{F_1}$ | W_{1max} | $\sin \beta_1$ | β_{1fl} | α |
| 600 | 5.65 | 18.2 | 10.85 | 18.2 | 0.31 | $161^\circ 50'$ | 18° |
| 1000 | 9.40 | 19.7 | 18.1 | 19.7 | .476 | $151^\circ 30'$ | $7^\circ 40'$ |
| 1400 | 13.2 | 21.8 | 25.3 | 25.3 | .605 | $142^\circ 50'$ | -1° |
| 2000 | 18.75 | 25.5 | 36.0 | 36.0 | .735 | $132^\circ 40'$ | $-11^\circ 0'$ |
| 2500 | 23.5 | 29.2 | 45.1 | 45.1 | .805 | $126^\circ 40'$ | $-17^\circ 30'$ |

TABLE 3

FLOW AT IMPELLER INLET

| a) First Stage Impeller | | | | | | |
|-------------------------|-------|----------------|----------------|----------|----------|-------|
| Q_{hr} | W_2 | $\cos \beta_2$ | $\sin \beta_2$ | C_{2m} | C_{2u} | C_2 |
| 600 | 17.1 | 0.865 | 0.502 | 8.55 | 27.2 | 28.5 |
| 1000 | 17.7 | .902 | .43 | 7.62 | 25.8 | 26.9 |
| 1400 | 20.7 | .86 | .51 | 10.55 | 24.1 | 26.3 |
| 2000 | 26.1 | .83 | .56 | 14.6 | 20.4 | 25.1 |
| 2500 | 30.8 | .804 | .595 | 18.3 | 17.1 | 25.0 |

| b) Second Stage Impeller | | | | | | |
|--------------------------|-------|----------------|----------------|----------|----------|-------|
| Q_{hr} | W_2 | $\cos \beta_2$ | $\sin \beta_2$ | C_{2m} | C_{2u} | C_2 |
| 600 | 18.2 | 0.758 | 0.652 | 11.8 | 28.1 | 30.5 |
| 1000 | 19.7 | .761 | .649 | 12.8 | 26.9 | 29.8 |
| 1400 | 20.6 | .834 | .556 | 11.47 | 24.8 | 27.3 |
| 2000 | 26.4 | .795 | .605 | 16.00 | 20.9 | 26.3 |
| 2500 | 31.9 | .779 | .625 | 19.90 | 17.1 | 26.2 |

TABLE 4

DETERMINATION OF TOTAL HYDRAULIC LOSSES IN IMPELLER

| a) First Stage Impeller | | | | | | |
|-------------------------|----------|-------|-----------------|----------------|---------------|------------------|
| Q_{hr} | H_{th} | C_2 | $H_{dyn\ comp}$ | $H_{st\ comp}$ | $H_{st\ exp}$ | ΔH_{imp} |
| 600 | 139 | 28.5 | 49.6 | 89.4 | 76.0 | 13.4 |
| 1000 | 132 | 26.9 | 44.3 | 87.7 | 74.0 | 13.7 |
| 1400 | 123 | 26.3 | 42.4 | 80.6 | 69.0 | 11.6 |
| 2000 | 104 | 25.1 | 38.5 | 65.5 | 53.0 | 12.5 |
| 2500 | 87 | 25.0 | 38.2 | 48.8 | 30.0 | 18.8 |

| b) Second Stage Impeller | | | | | | |
|--------------------------|----------|-------|-----------------|----------------|---------------|------------------|
| Q_{hr} | H_{th} | C_2 | $H_{dyn\ comp}$ | $H_{st\ comp}$ | $H_{st\ exp}$ | ΔH_{imp} |
| 600 | 148.0 | 30.5 | 57.0 | 86.0 | 72.0 | 14.0 |
| 1000 | 137.5 | 29.8 | 54.0 | 83.5 | 69.0 | 14.5 |
| 1400 | 127.0 | 27.3 | 45.5 | 81.5 | 64.0 | 17.5 |
| 2000 | 106.5 | 26.3 | 42.2 | 64.3 | 55.0 | 9.3 |
| 2500 | 87.5 | 26.2 | 42.0 | 45.5 | 37.5 | 8.5 |

TABLE 6

FLOW AT VANELESS DIFFUSER INLET

| a) First Stage | | | | | | | | |
|----------------|----------------------|-----------------------|-----------|----------|----------|-------|-----------------|------------|
| Q_{hr} | $H_{st \text{ imp}}$ | $H_{dyn \text{ imp}}$ | H_{dif} | C_{3u} | C_{3m} | C_3 | $\tan \alpha_3$ | α_3 |
| 600 | 76.0 | 49.6 | 125.6 | 27.2 | 4.09 | 27.5 | 0.1504 | 8°35 |
| 1000 | 74.0 | 44.3 | 118.3 | 25.8 | 6.80 | 26.7 | .264 | 14°50 |
| 1400 | 69.0 | 42.4 | 111.4 | 24.1 | 9.55 | 25.9 | .396 | 21°40 |
| 2000 | 53.0 | 38.5 | 91.5 | 20.4 | 13.6 | 24.5 | .666 | 33°40 |
| 2500 | 30.0 | 38.2 | 68.2 | 17.1 | 17.0 | 24.1 | .995 | 44°50 |

| b) Second Stage | | | | | | | | |
|-----------------|----------|-----------|-----------|----------|----------|-------|-----------------|------------|
| Q_{hr} | H_{st} | H_{dyn} | H_{dif} | C_{3u} | C_{3m} | C_3 | $\tan \alpha_3$ | α_3 |
| 600 | 72 | 57 | 129 | 28.1 | 4.43 | 28.4 | 0.158 | 9°-- |
| 1000 | 69 | 54 | 123 | 26.9 | 7.38 | 27.9 | .274 | 15°20 |
| 1400 | 64 | 45.5 | 109.5 | 24.8 | 10.35 | 26.9 | .417 | 22°40 |
| 2000 | 55 | 42.2 | 97.2 | 20.9 | 14.7 | 25.6 | .704 | 35°10 |
| 2500 | 37 | 42.0 | 79.0 | 17.1 | 18.4 | 25.2 | 1.075 | 46°50 |

TABLE 9

COMPUTED VALUES OF STATIC HEAD AT OUTLET OF STAGE

| a) First Stage | | | | | | | | |
|----------------|-----------|-------------------|---------------------|------------------|---------------------|-------------|--------------------------|------------------------|
| Q_{hr} | H_{dif} | ΔH_{defl} | ΔH_{impact} | $\Delta H_{g v}$ | ΔH_{outlet} | H_{stage} | $H_{dyn \text{ outlet}}$ | $H_{st \text{ stage}}$ |
| 600 | 106.2 | 0.86 | 2.38 | 3.8 | 0.12 | 98.6 | 1.6 | 97.0 |
| 1000 | 107.4 | 2.4 | 3.05 | 3.1 | 1.72 | 97.1 | 4.3 | 92.8 |
| 1400 | 103.1 | 4.7 | 3.19 | 1.6 | 3.37 | 90.2 | 8.5 | 81.7 |
| 2000 | 83.5 | 9.5 | 2.81 | .05 | 6.9 | 64.2 | 17.2 | 47.0 |
| 2500 | 59.4 | 14.7 | 2.6 | ---- | 10.8 | 31.3 | 27.0 | 4.3 |

| b) Second Stage | | | | | | | | |
|-----------------|-----------|-------------------|---------------------|------------------|---------------------|-------------|--------------------------|------------------------|
| Q_{hr} | H_{dif} | ΔH_{defl} | ΔH_{impact} | $\Delta H_{g v}$ | ΔH_{outlet} | H_{stage} | $H_{dyn \text{ outlet}}$ | $H_{st \text{ stage}}$ |
| 600 | 91.05 | 1.05 | 1.72 | 2.35 | 0.62 | 85.3 | 1.6 | 83.7 |
| 1000 | 95.5 | 2.8 | 2.51 | 2.13 | 1.72 | 86.3 | 4.3 | 82.0 |
| 1400 | 95.1 | 5.5 | 2.73 | 1.02 | 3.37 | 82.5 | 8.5 | 74.0 |
| 2000 | 82.5 | 11.0 | 2.3 | ---- | 6.9 | 62.0 | 17.2 | 44.8 |
| 2500 | 63.8 | 17.3 | 2.6 | ---- | 10.8 | 33.4 | 27.0 | 6.4 |

Table 7

Flow at vaneless diffuser outlet for various values of the friction coefficient λ .
(a) Plane diffuser of first stage..

| Q_{hr} | C_m | $\lambda = 0,05$ | | | | | $\lambda = 0,1$ | | | | | $\lambda = 0,15$ | | | | |
|----------|-------|------------------|----------|-------|------------------------------|-----------------|-----------------|----------|-------|------------------------------|-----------------|------------------|----------|-------|------------------------------|-----------------|
| | | α_a | C_{ua} | C_a | $\rho \cdot \frac{C_a^2}{2}$ | ΔH_{fr} | α_a | C_{ua} | C_a | $\rho \cdot \frac{C_a^2}{2}$ | ΔH_{fr} | α_a | C_{ua} | C_a | $\rho \cdot \frac{C_a^2}{2}$ | ΔH_{fr} |
| 600 | 2,65 | 10°58' | 13,7 | 13,95 | 11,9 | 11,2 | 13°10' | 11,35 | 11,6 | 8,2 | 19,9 | 15°45' | 9,42 | 9,82 | 5,9 | 24,7 |
| 1000 | 4,41 | 17°10' | 14,35 | 14,05 | 12,6 | 7,2 | 19°20' | 12,6 | 13,3 | 10,4 | 13,2 | 21°50' | 11,0 | 11,85 | 8,6 | 17,4 |
| 1400 | 6,19 | 24°55' | 13,35 | 14,65 | 13,1 | 4,88 | 26°— | 12,7 | 14,1 | 12,1 | 9,3 | 28°20' | 11,45 | 13,0 | 10,3 | 13,3 |
| 2000 | 8,8 | 35°45' | 12,2 | 15,1 | 13,9 | 3,29 | 38°— | 11,3 | 14,3 | 12,5 | 6,8 | 39°40' | 10,62 | 13,8 | 11,6 | 9,24 |
| 2500 | 11,05 | 46°40' | 10,45 | 15,2 | 14,1 | 2,61 | 48°— | 9,9 | 14,8 | 13,4 | 5,15 | 49°50' | 9,3 | 14,4 | 12,7 | 7,5 |

(b) Plane diffuser of second stage.

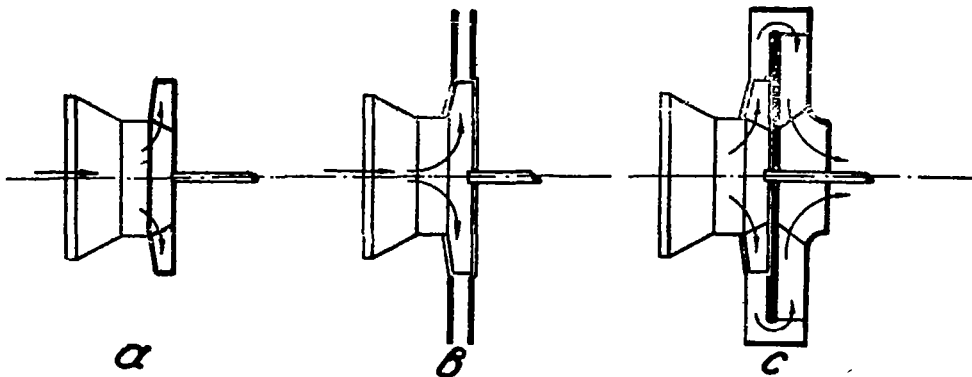
| Q_{hr} | C_m | $\lambda = 0,05$ | | | | | $\lambda = 0,1$ | | | | | $\lambda = 0,15$ | | | | |
|----------|-------|------------------|----------|-------|------------------------------|-----------------|-----------------|----------|-------|------------------------------|-----------------|------------------|----------|-------|------------------------------|-----------------|
| | | α_a | C_{ua} | C_a | $\rho \cdot \frac{C_a^2}{2}$ | ΔH_{fr} | α_a | C_{ua} | C_a | $\rho \cdot \frac{C_a^2}{2}$ | ΔH_{fr} | α_a | C_{ua} | C_a | $\rho \cdot \frac{C_a^2}{2}$ | ΔH_{fr} |
| 600 | 2,86 | 11°27' | 14,6 | 14,4 | 12,6 | 12,4 | 14°— | 11,6 | 11,85 | 8,6 | 22,0 | 16°40' | 9,58 | 9,96 | 6,05 | 27,7 |
| 1000 | 4,76 | 17°50' | 15,3 | 15,6 | 14,8 | 9,35 | 20°15' | 13,0 | 13,88 | 11,8 | 15,0 | 22°50' | 11,35 | 12,5 | 9,5 | 19,9 |
| 1400 | 6,7 | 24°50' | 14,9 | 15,95 | 15,5 | 5,9 | 17°20' | 13,0 | 14,4 | 12,6 | 10,6 | 29°50' | 11,65 | 13,5 | 11,1 | 15,0 |
| 2000 | 9,53 | 37°10' | 13,0 | 15,8 | 15,2 | 3,65 | 39°15' | 11,7 | 15,1 | 13,8 | 7,0 | 41°30' | 10,7 | 14,3 | 12,5 | 10,3 |
| 2500 | 11,9 | 48°40' | 10,9 | 15,9 | 15,4 | 3,05 | 50°10' | 9,9 | 15,5 | 14,7 | 5,7 | 52°10' | 9,2 | 15,05 | 13,8 | 8,56 |

Table 8
 Static head at diffuser outlet for various values of the friction coefficient λ .
 (a) Plane diffuser of first stage.

| Q_{hr} | $H_{st\ exp}$ | H_{dif} | ΔH_{impact} | $\lambda = 0,05$ | | | $\lambda = 0,1$ | | | $\lambda = 0,15$ | | |
|----------|---------------|-----------|---------------------|------------------|-----------|----------------|-----------------|-----------|----------------|------------------|-----------|----------------|
| | | | | ΔH_{fr} | H_{dyn} | $H_{st\ comp}$ | ΔH_{fr} | H_{dyn} | $H_{st\ comp}$ | ΔH_{fr} | H_{dyn} | $H_{st\ comp}$ |
| 600 | 98,0 | 125,6 | 1,21 | 11,2 | 11,9 | 101,3 | 19,4 | 8,2 | 96,25 | 24,7 | 5,9 | 93,8 |
| 1000 | 97,0 | 118,3 | 0,41 | 7,2 | 12,6 | 98,5 | 13,2 | 10,4 | 94,7 | 17,4 | 8,6 | 92,3 |
| 1400 | 91,0 | 111,4 | 0,06 | 4,88 | 13,1 | 93,4 | 9,3 | 12,1 | 90,0 | 13,3 | 10,3 | 87,8 |
| 2000 | 71,0 | 91,5 | 0,06 | 3,29 | 13,9 | 74,3 | 6,8 | 12,5 | 72,0 | 9,24 | 11,6 | 70,7 |
| 2500 | 46,0 | 68,2 | 0,05 | 2,61 | 14,1 | 51,5 | 5,15 | 13,4 | 49,6 | 7,5 | 12,7 | 48,0 |

(b) Plane diffuser of second stage.

| Q_{hr} | $H_{st\ exp}$ | H_{dif} | ΔH_{impact} | $\lambda = 0,05$ | | | $\lambda = 0,1$ | | | $\lambda = 0,15$ | | |
|----------|---------------|-----------|---------------------|------------------|-----------|----------------|-----------------|-----------|----------------|------------------|-----------|----------------|
| | | | | ΔH_{fr} | H_{dyn} | $H_{st\ comp}$ | ΔH_{fr} | H_{dyn} | $H_{st\ comp}$ | ΔH_{fr} | H_{dyn} | $H_{st\ comp}$ |
| 600 | 85,0 | 129,0 | 3,3 | 12,4 | 12,6 | 100,7 | 22,0 | 8,6 | 95,1 | 27,7 | 6,05 | 92,0 |
| 1000 | 86,0 | 123,0 | 1,78 | 9,35 | 14,8 | 97,0 | 15,0 | 11,8 | 94,4 | 19,9 | 9,5 | 91,8 |
| 1400 | 84,0 | 109,5 | 0,07 | 5,9 | 15,5 | 88,1 | 10,6 | 12,6 | 86,3 | 14,6 | 11,1 | 83,7 |
| 2000 | 70,0* | 97,2 | 0,06 | 3,65 | 15,2 | 78,4 | 7,0 | 13,8 | 76,3 | 10,3 | 12,5 | 74,4 |
| 2500 | 50,0 | 79,0 | 0,06 | 3,05 | 15,4 | 60,55 | 5,7 | 14,7 | 58,6 | 8,56 | 13,8 | 56,8 |



a Isolated impeller b Vaneless diffuser c Reversing guide vanes

Figure 1.- Scheme of successive investigation of the individual elements of a turbo blower.

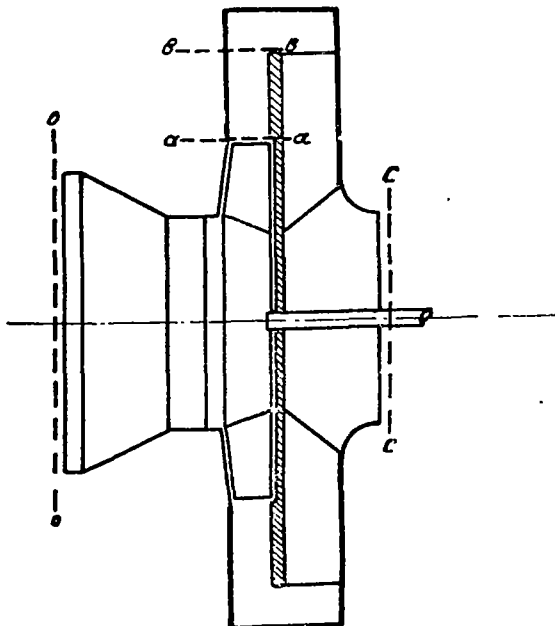


Figure 2.^s Determination of the general value of the losses in the individual elements of the turbo blower.

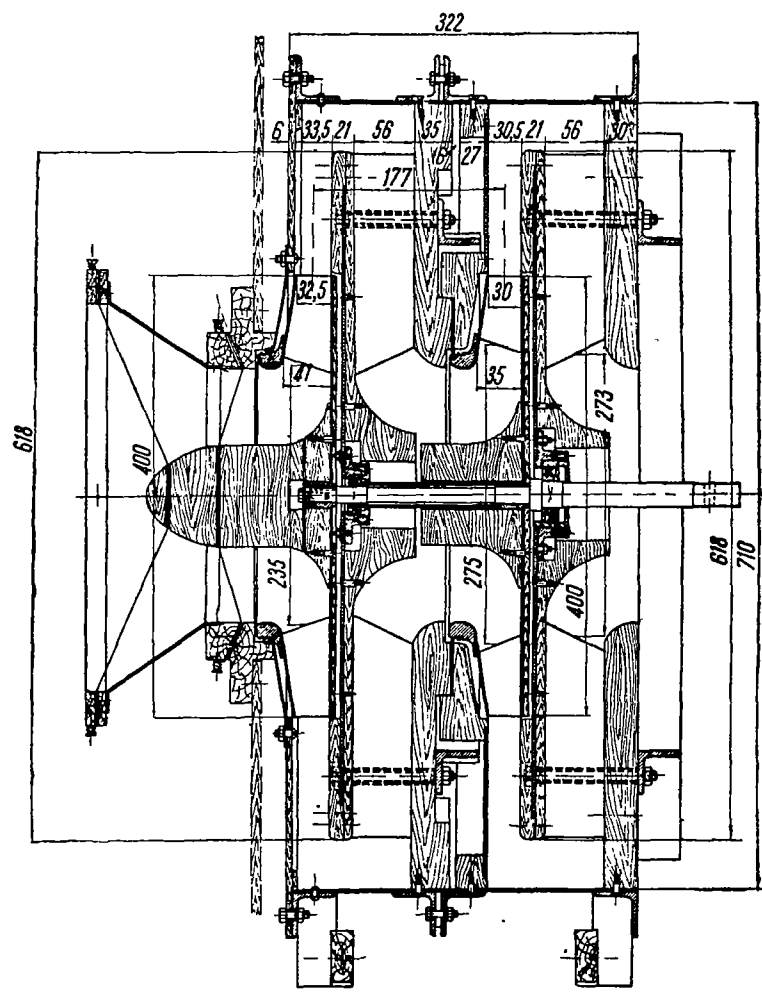
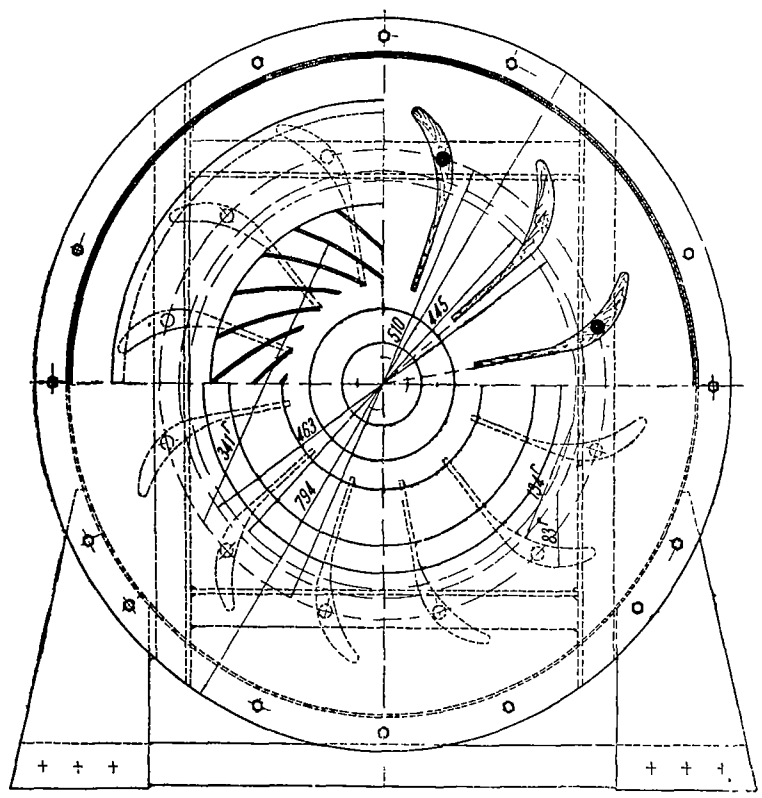


Figure 3.- Model of a two-stage turbo blower.

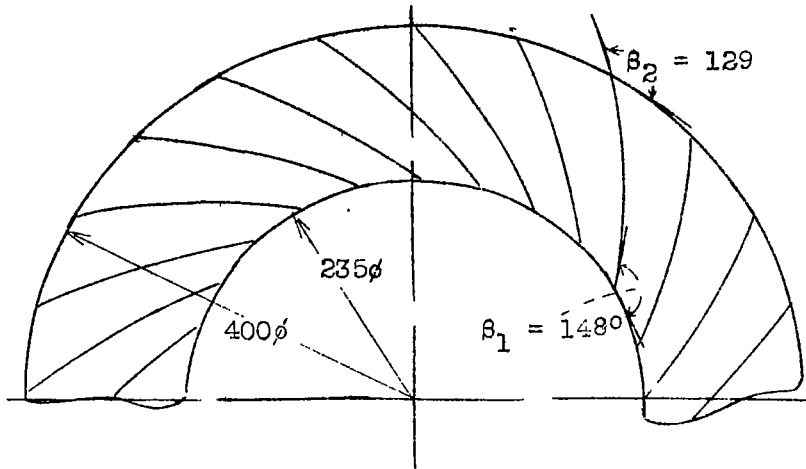


Figure 4a.- Aerodynamic scheme of impeller of first stage of turbo blower.

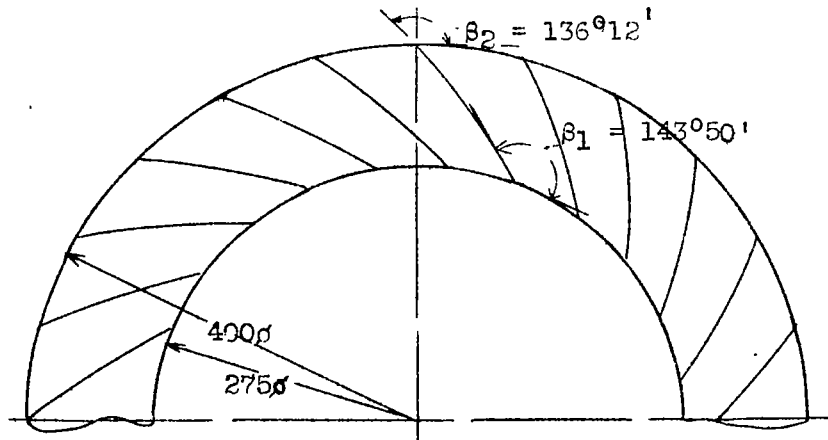


Figure 4b.- Aerodynamic scheme of impeller of second stage of turbo blower.

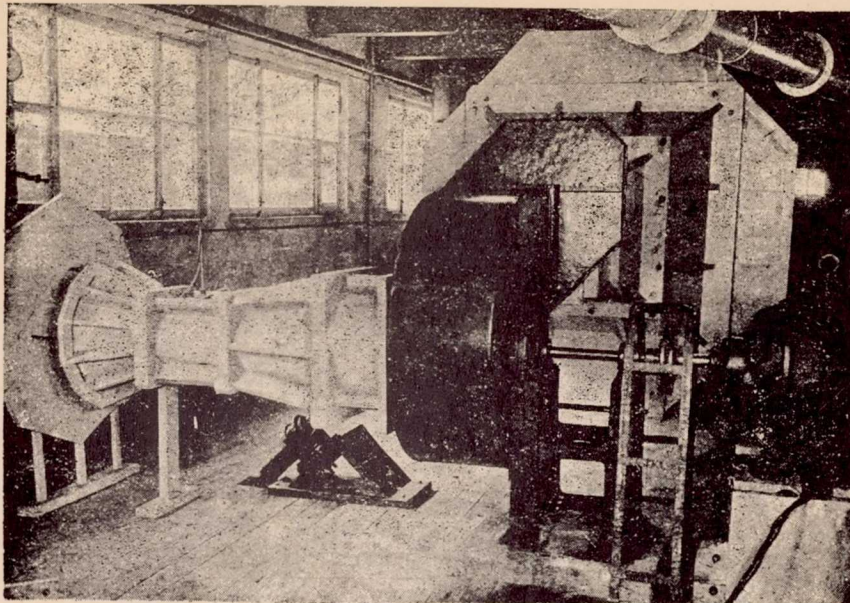


Figure 5.- View of blower in suction test chamber.



Figure 13.- Photograph of flow through impeller of centrifugal pump (Thoma and Fisher).



Figure 14.- Sketch of flow through impeller for positive angles of attack.

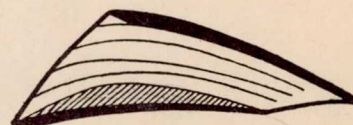
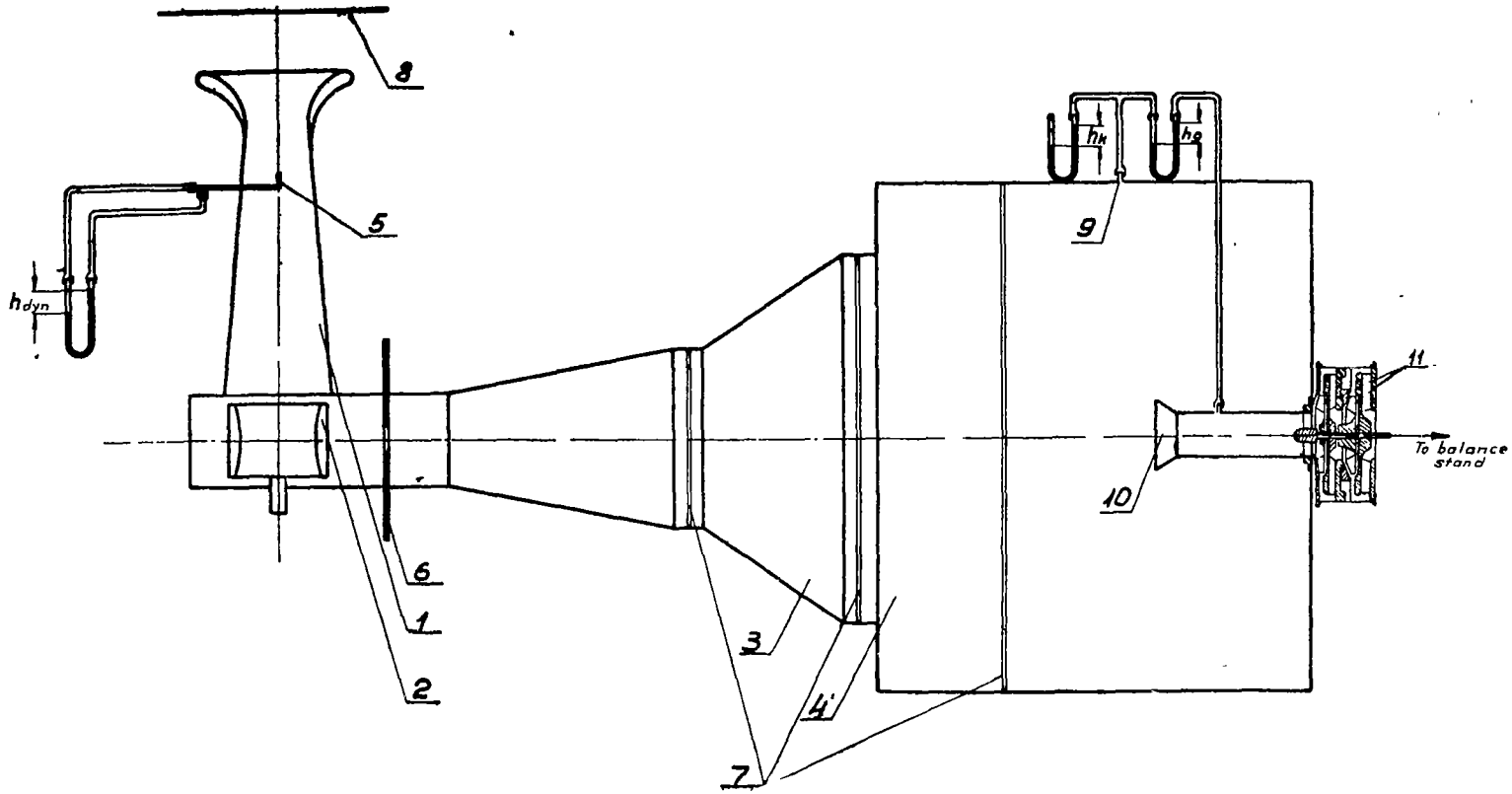


Figure 15.- Sketch of flow through impeller for negative angles of attack.



- | | | | | | | | |
|---|------------|---|----------------------|---|---------------------------------|----|-------------------|
| 1 | Entry part | 4 | Low pressure chamber | 7 | Screens | 10 | Conical collector |
| 2 | Fan | 5 | Pitot tube | 8 | Screen | 11 | Model blower |
| 3 | Diffuser | 6 | Throttle | 9 | Tube for measuring H chamber | | |

Figure 6.- Sketch of test set-up of model two-stage blower in chamber.

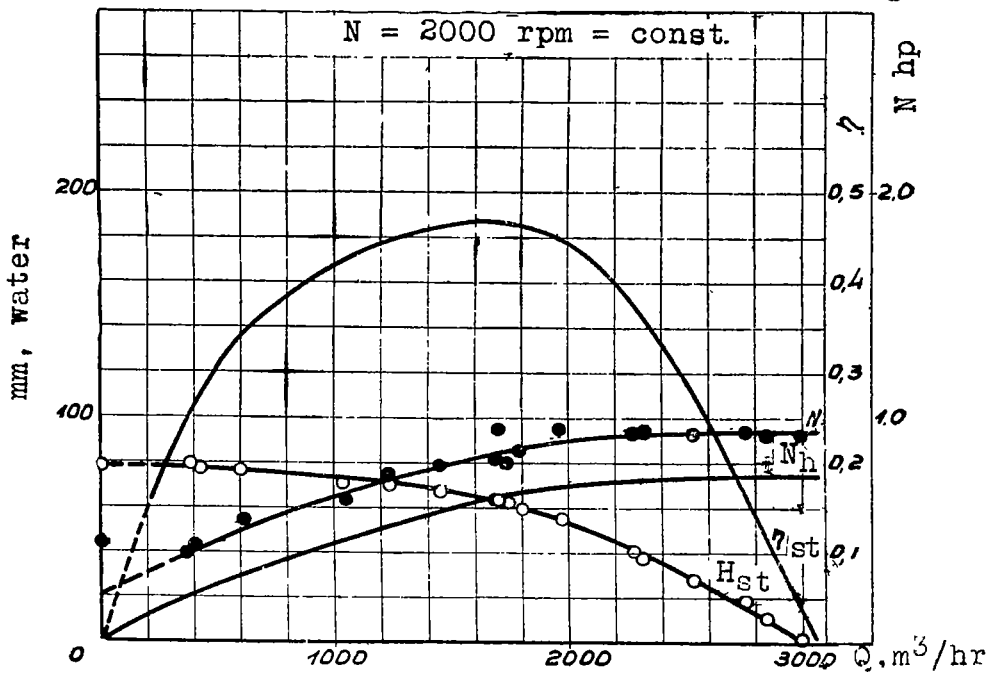


Figure 7a.- Impeller characteristics of first stage of turbo blower.

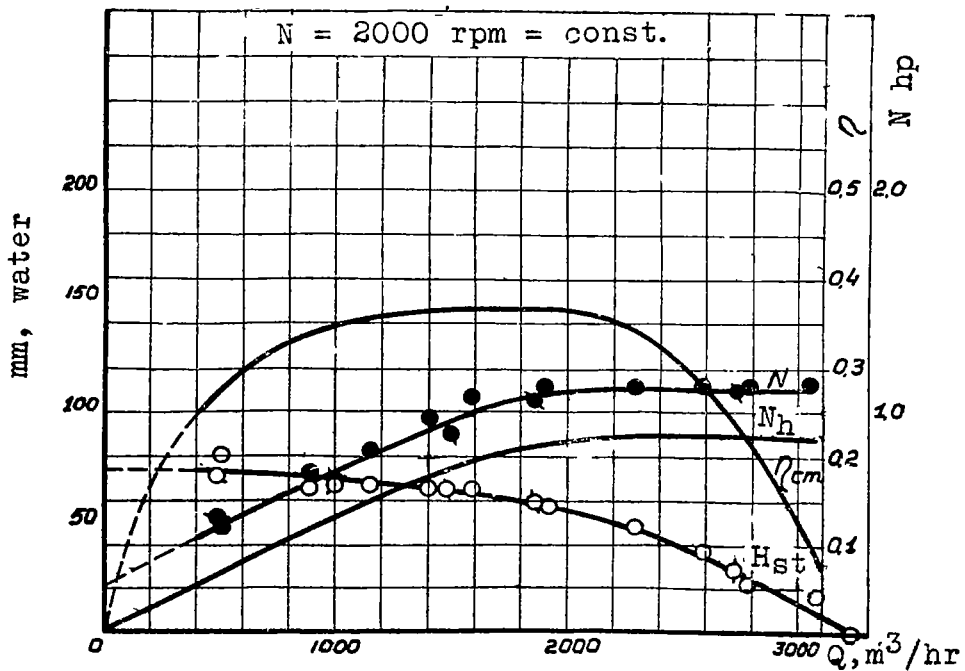


Figure 7b.- Impeller characteristics of second stage of turbo blower.

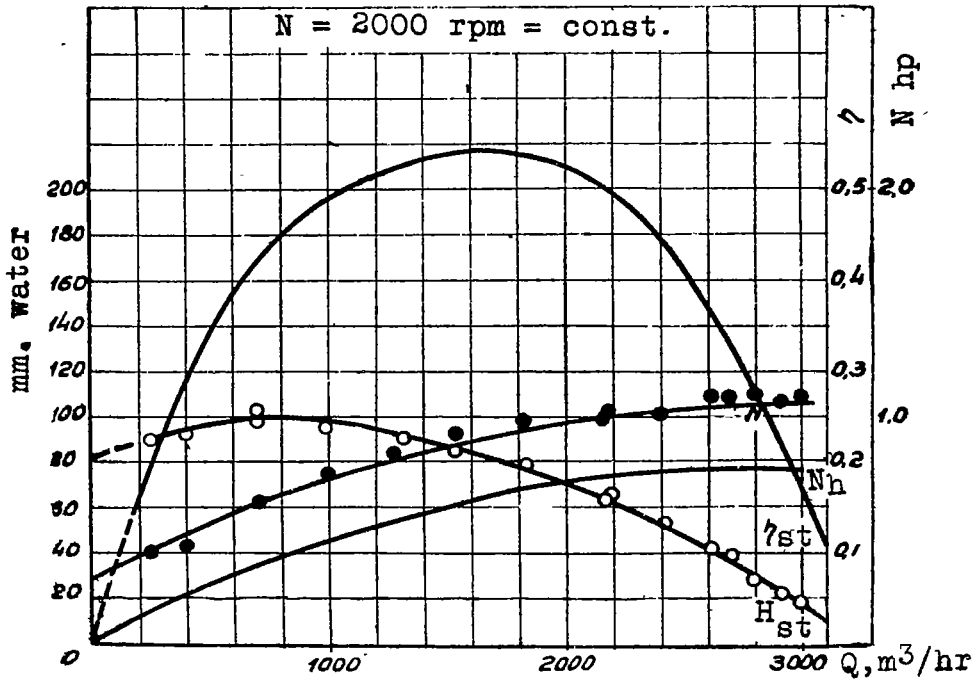


Figure 8a.- Characteristics of impeller of first stage of turbo blower with vaneless diffuser behind impeller.

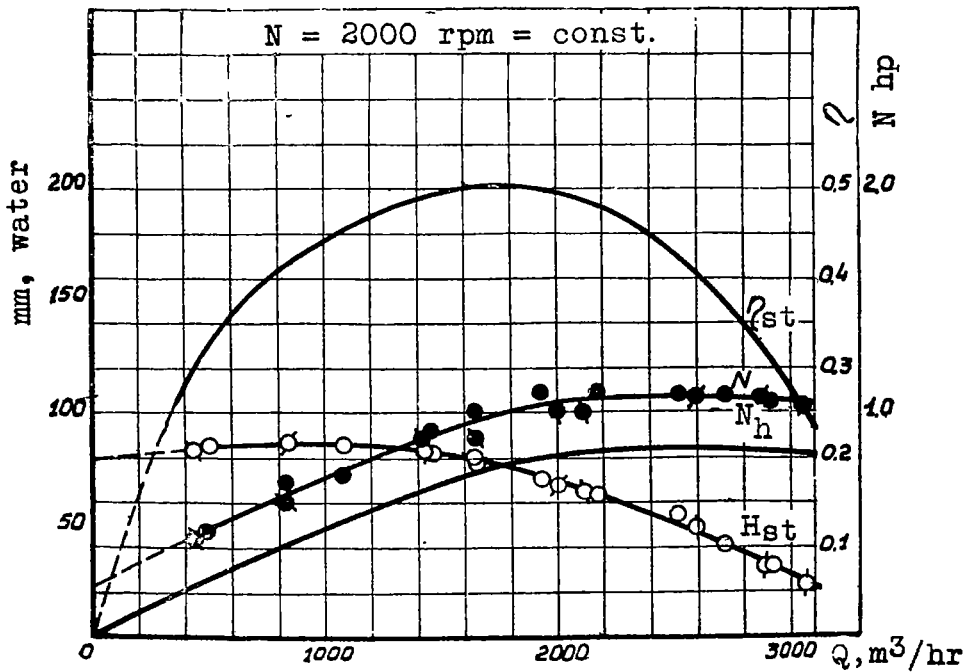


Figure 8b.- Characteristics of impeller of second stage of turbo blower with vaneless diffuser behind impeller.

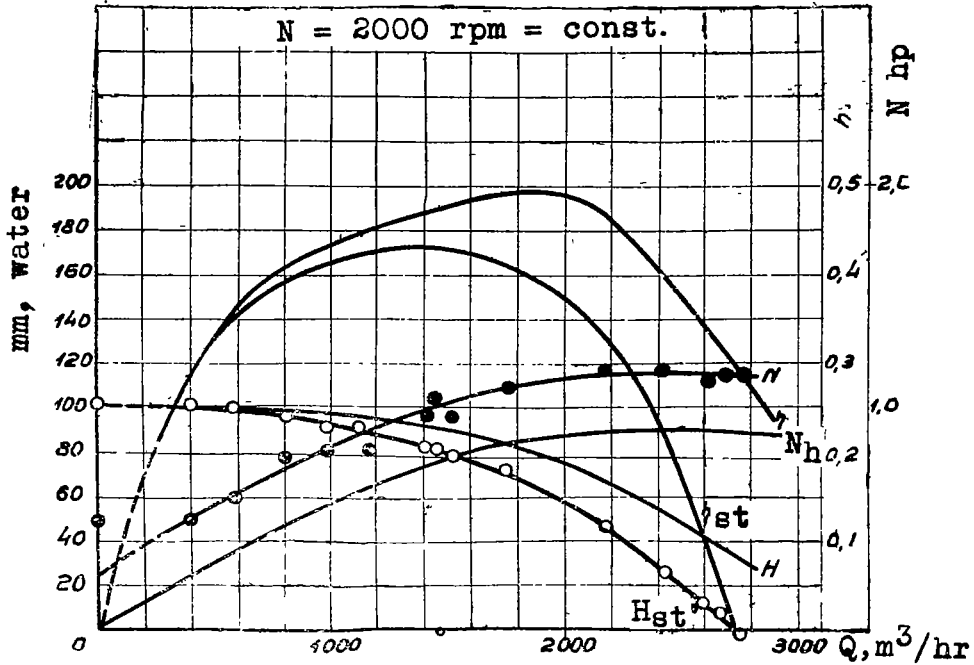


Figure 9a.- Characteristics of first stage of turbo blower (impeller, vaneless diffuser, reversing guide vanes).

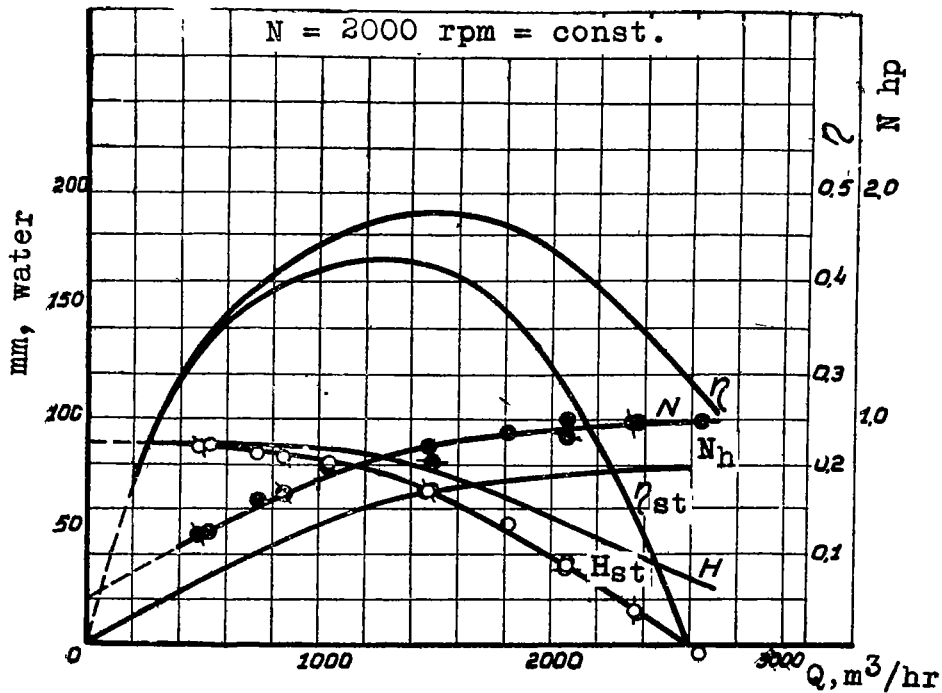


Figure 9b.- Characteristics of second stage of turbo blower (impeller, vaneless diffuser, reversing guide vanes.)

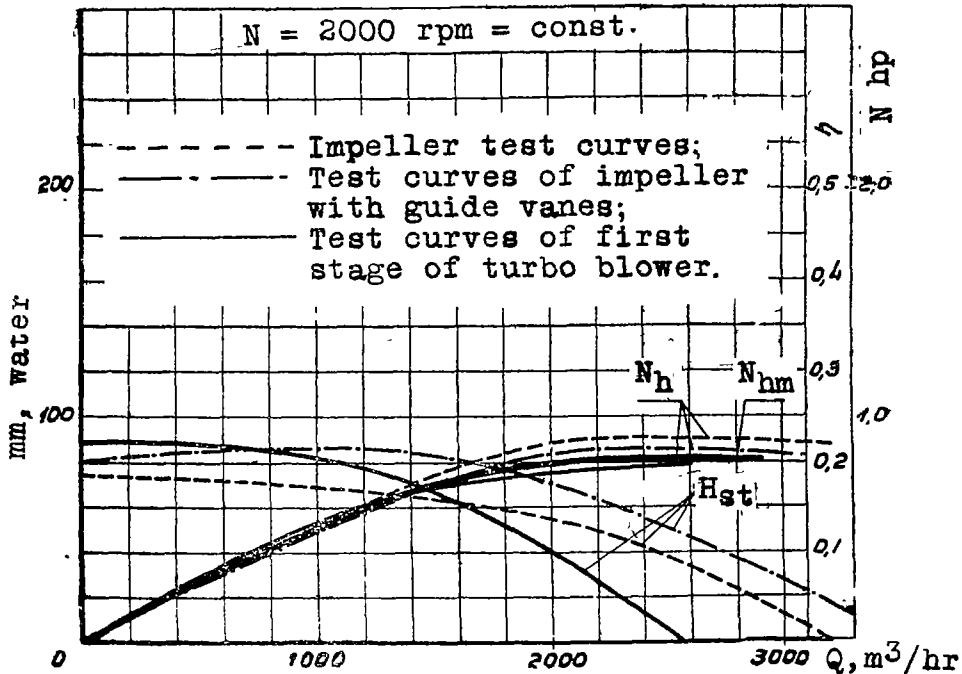


Figure 10a. Combined curves of static pressure heads H_{st} and hydraulic power N_h obtained in testing the individual elements of the first stage of the turbo blower.

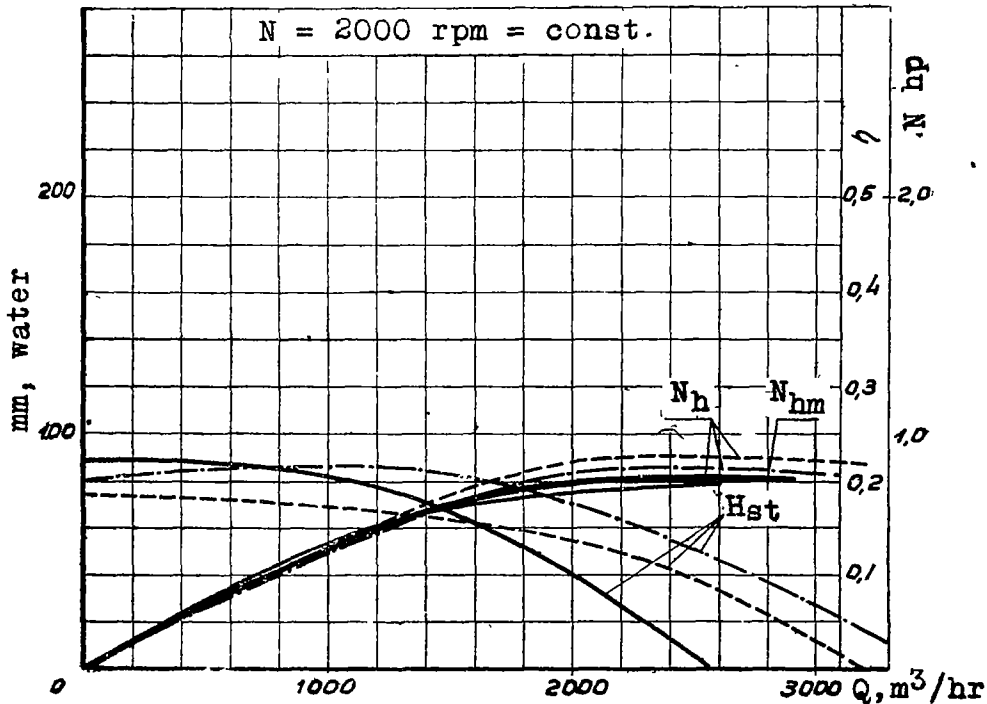


Figure 10b.- Combined curves of static pressure heads H_{st} and hydraulic power N_h obtained in testing the individual elements of the second stage of the turbo blower (notation the same as for figure 10a).

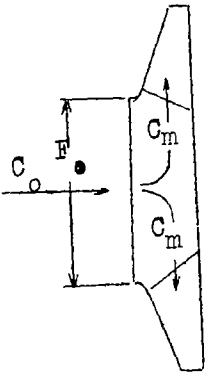


Figure 11.- Flow at impeller inlet.

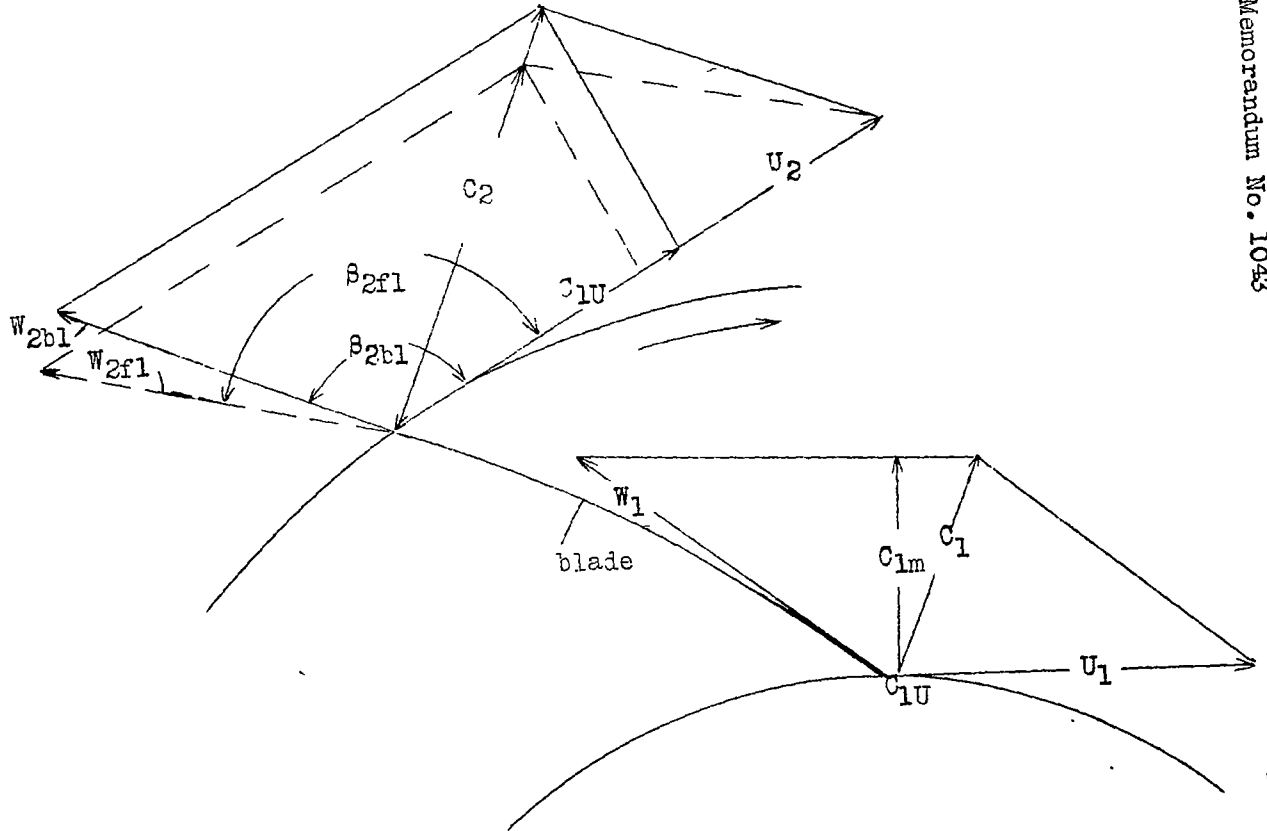


Figure 12.- Velocity diagrams at inlet and outlet of impeller.

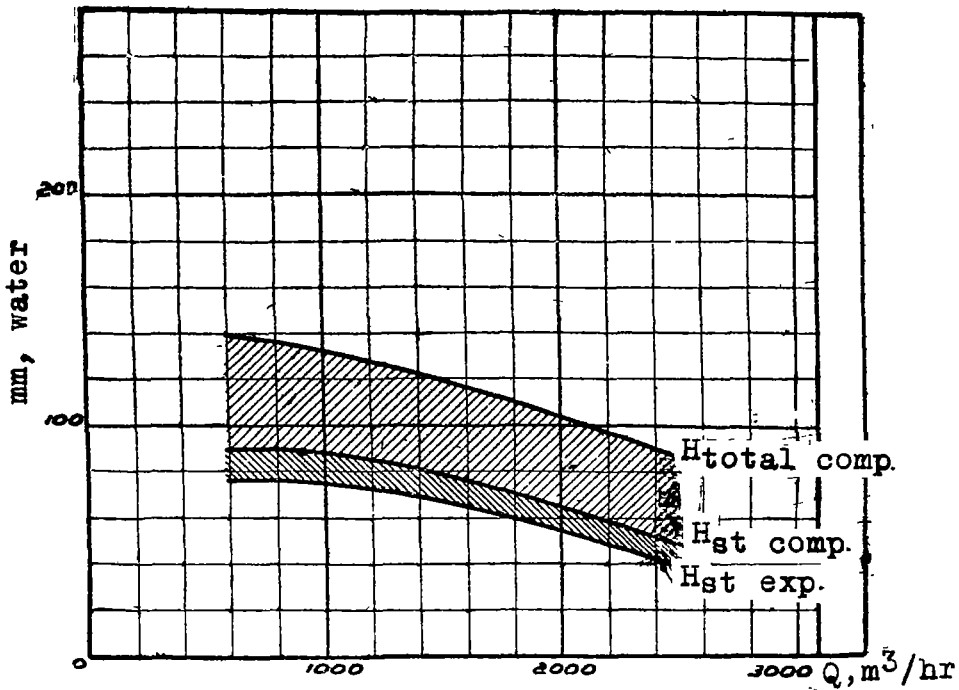


Figure 16a.- Hydraulic losses in the impeller of the first stage.

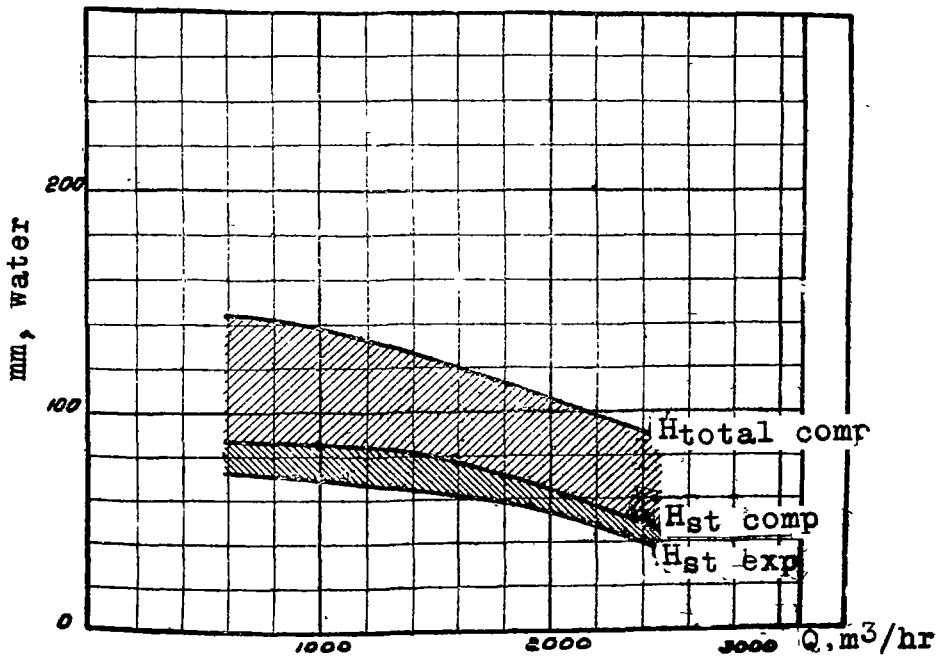


Figure 16b.- Hydraulic losses in the impeller of the second stage.

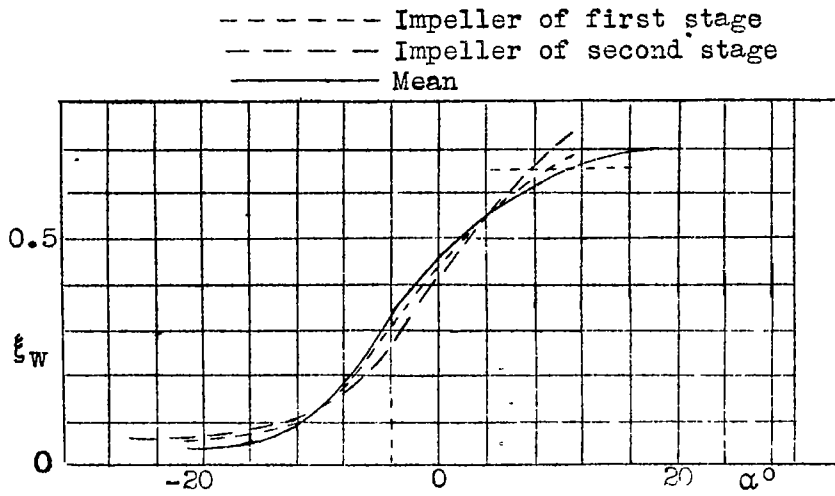


Figure 17.- Dependence of the loss coefficient for the flow through the impeller ξ_w on the angle of attack α .

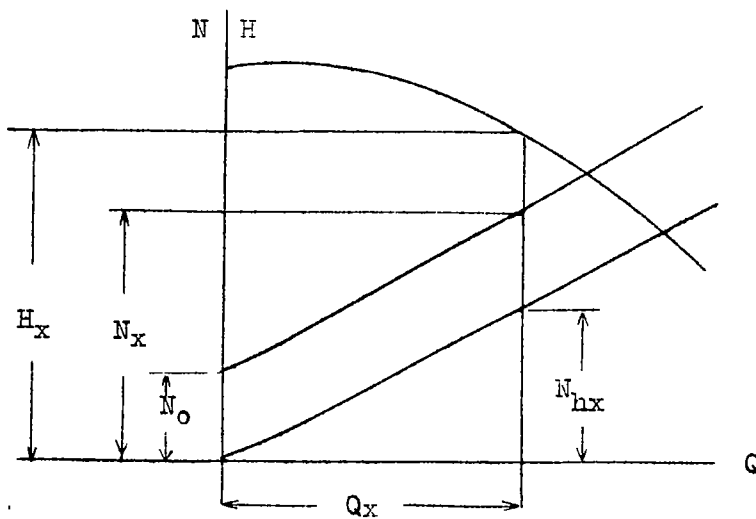


Figure 24.

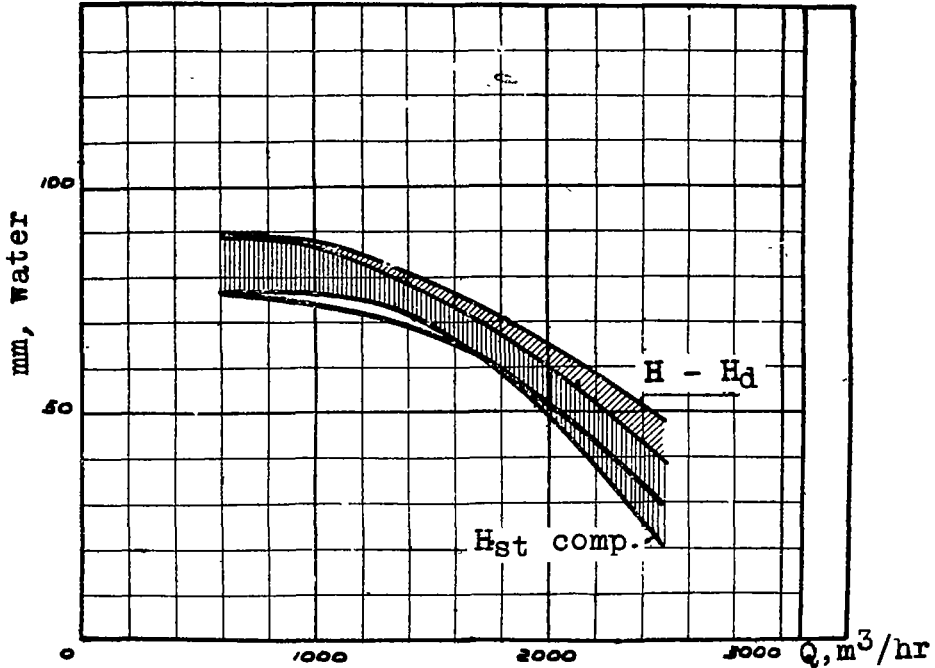


Figure 18a.- Computed value of static head at exit of impeller of first stage.

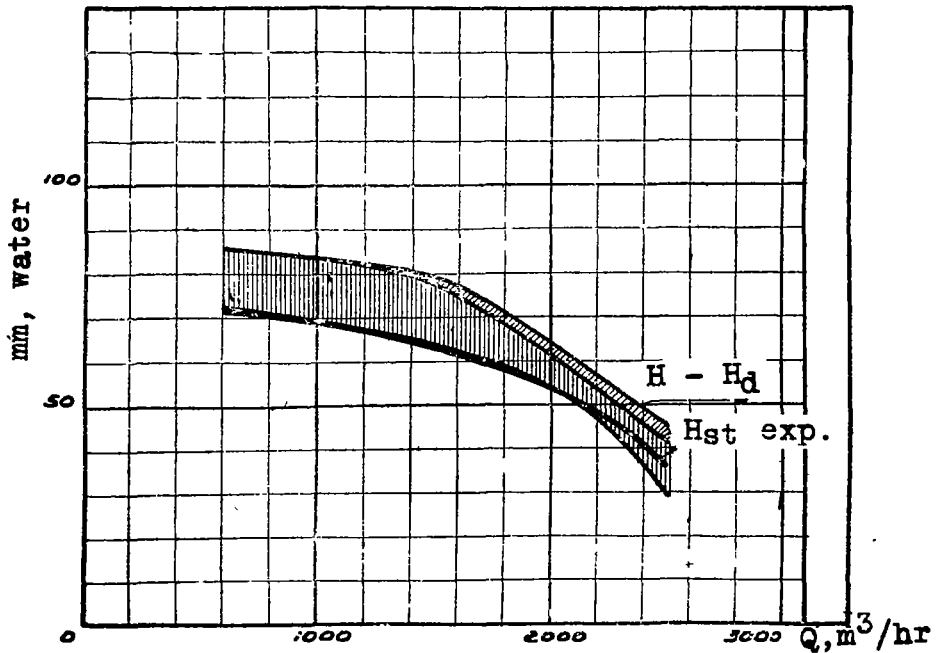


Figure 18b.- Computed value of static head at exit of impeller of second stage.

Table 5
Computed static head at impeller outlet

a) Impeller of first stage

| Q_{hr} | H_T | H_d | ΔH_c | ΔH_w | Hst comp. | Hst exp. |
|----------|-------|-------|--------------|--------------|-----------|----------|
| 600 | 139 | 49,6 | 0,46 | 12,1 | 76,9 | 76,0 |
| 1000 | 132 | 44,3 | 1,28 | 12,1 | 74,3 | 74,0 |
| 1400 | 123 | 42,4 | 2,5 | 6,75 | 71,3 | 69,0 |
| 2000 | 104 | 38,5 | 5,1 | 12,6 | 47,8 | 53,0 |
| 2500 | 87 | 38,2 | 7,94 | 19,8 | 21,0 | 30,0 |

b) Impeller of second stage

| Q_{hr} | H_T | H_d | ΔH_c | ΔH_w | Hst comp. | Hst exp. |
|----------|-------|-------|--------------|--------------|-----------|----------|
| 600 | 143 | 57,0 | 0,2 | 13,8 | 72,0 | 72,0 |
| 1000 | 137,5 | 54,0 | 0,54 | 15,2 | 67,8 | 69,0 |
| 1400 | 127,0 | 45,5 | 1,06 | 15,6 | 64,9 | 64,0 |
| 2000 | 106,5 | 42,2 | 2,15 | 7,9 | 54,2 | 55,0 |
| 2500 | 87,5 | 42,0 | 3,37 | 12,4 | 29,7 | 37,0 |

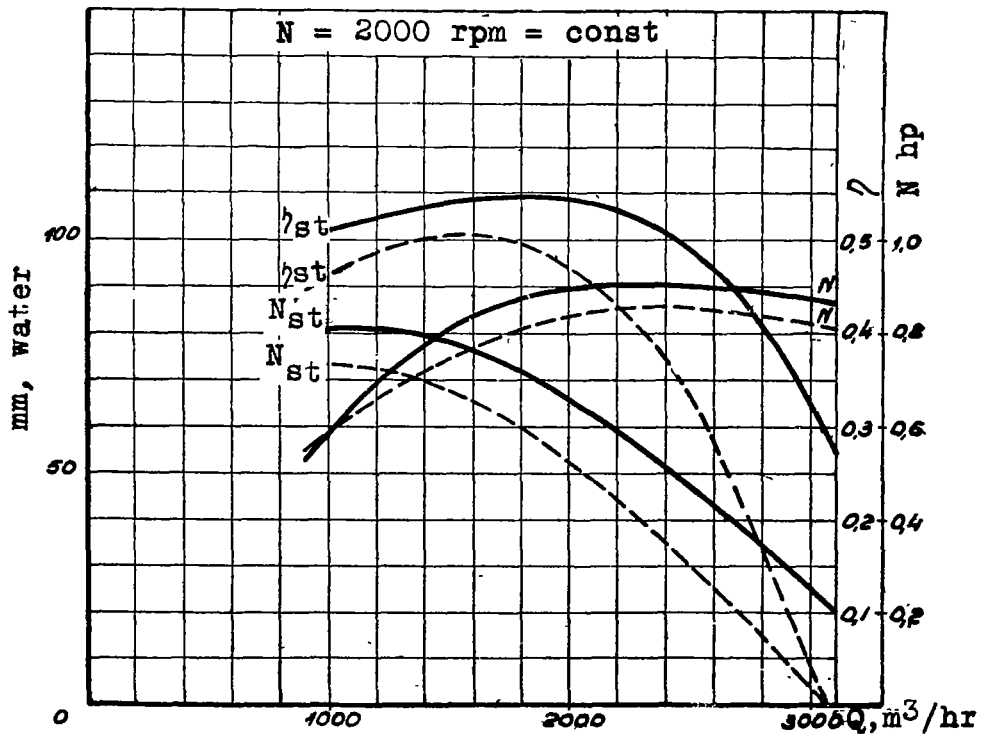


Figure 19.- Effect of shortening the blades at the impeller inlet on the performance of the model impeller of one of the LMZ turbo blowers.

----- Test curves with normal blades;
 _____ Test curves with shortened blades.

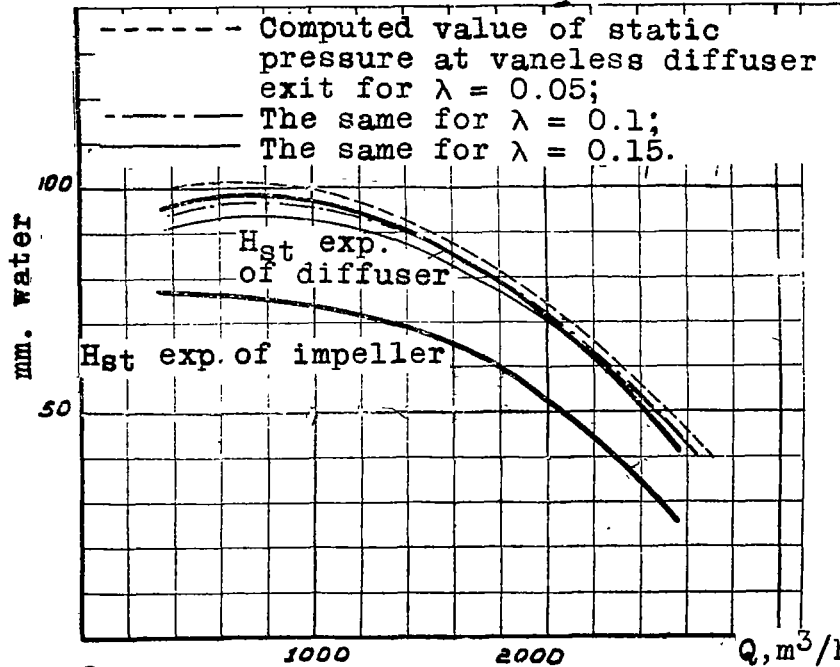


Figure 20a.- Computed values of the static pressures at the outlet of the vaneless diffuser of the first stage for various values of the friction coefficient. 1- test value of static pressure at impeller exit; 2- test value of static pressure at vaneless diffuser exit.

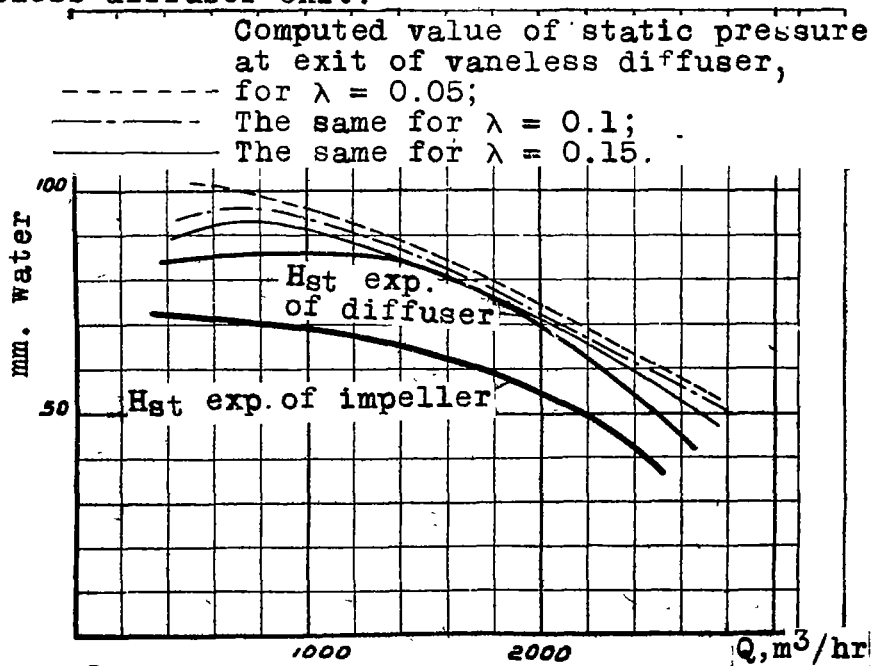


Figure 20b.- Computed values of the static pressures at the exit of the vaneless diffuser of the second stage for various values of the friction coefficient. 1- test value of the static pressure at the impeller exit; 2- test value of static pressure at vaneless diffuser exit,

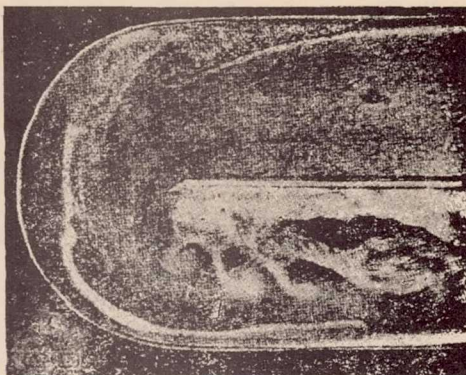


Figure 21.- Flow through channel deflected by 180° (Frey).

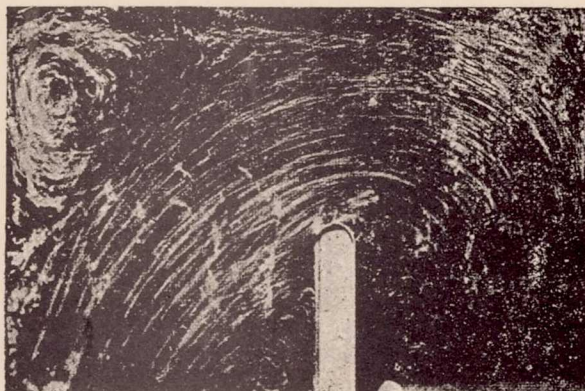


Figure 22.- Flow through channel deflected by 180° and with varying cross-section after deflection.

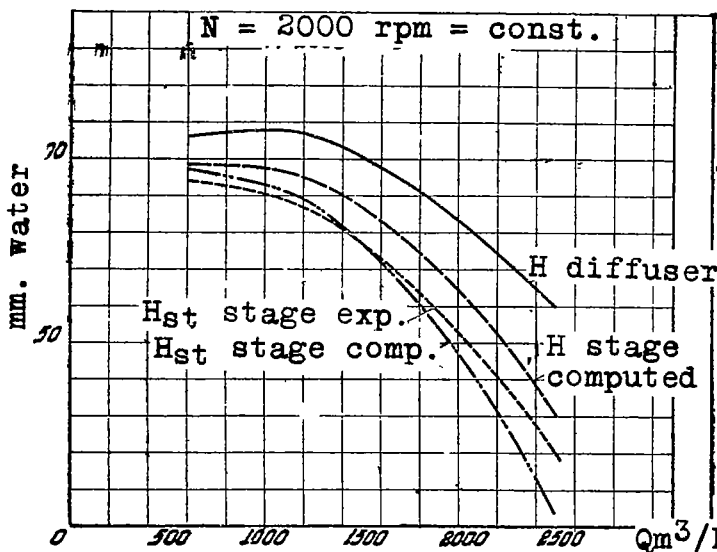


Figure 23a.- Computed values of total and static heads at outlet of first stage.
 ————— computed value of total head at vaneless diffuser outlet, - - - - - computed value of total head at outlet of first stage; ———— computed value of static head at outlet of stage; ———— test value of static head at outlet of stage.

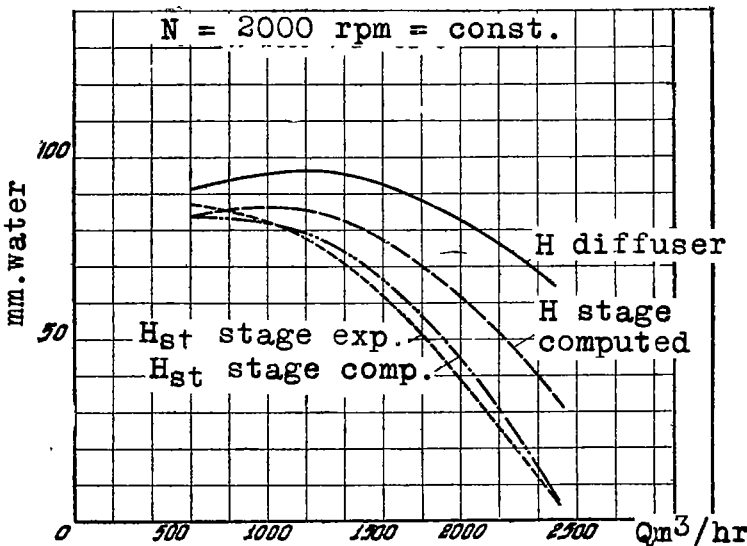


Figure 23b.- Computed values of total and static heads at outlet of second stage.

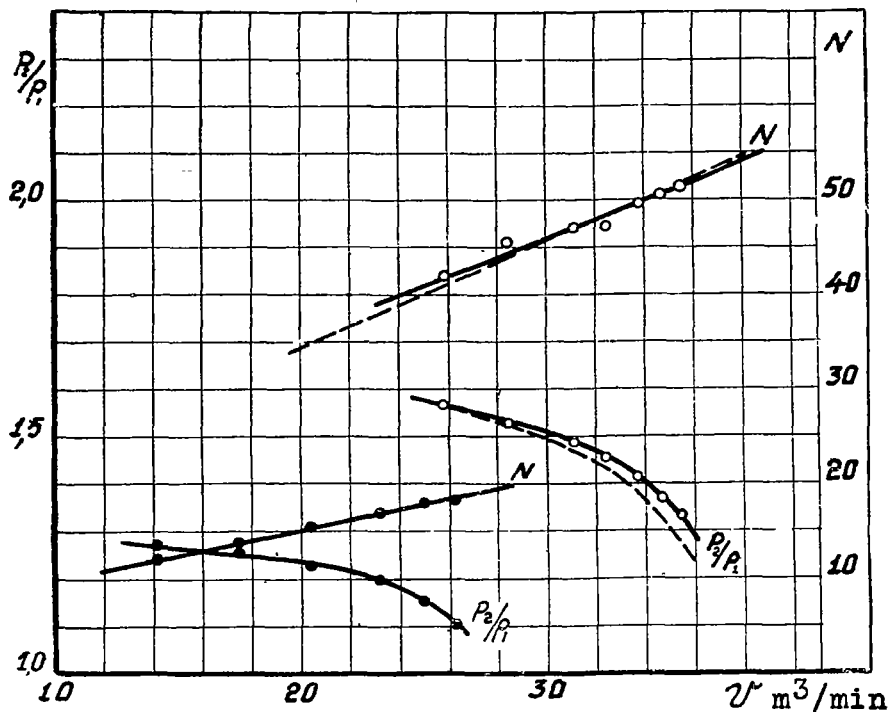


Figure 25a.- Guide vanes set at 12°

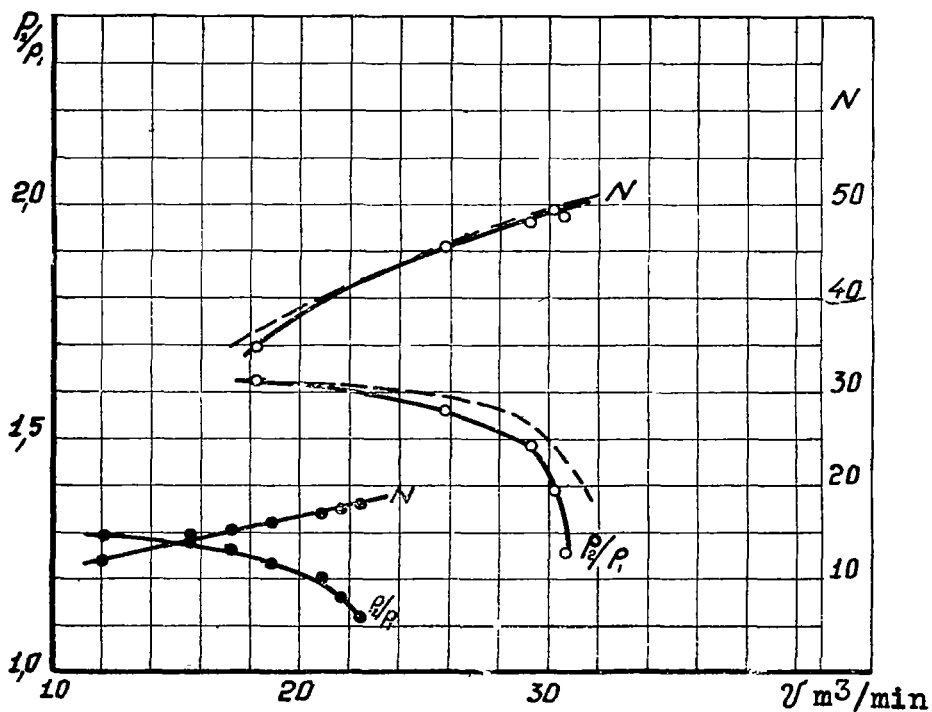


Figure 25b.- Guide vanes set at 17° .

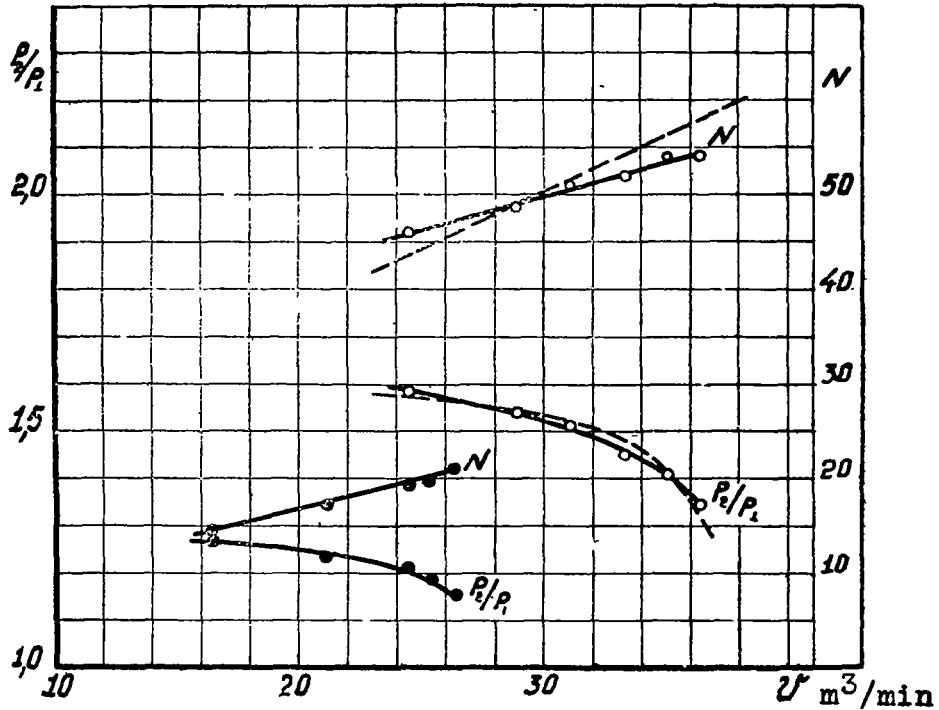


Figure 25c.- Guide vanes set at 22°.

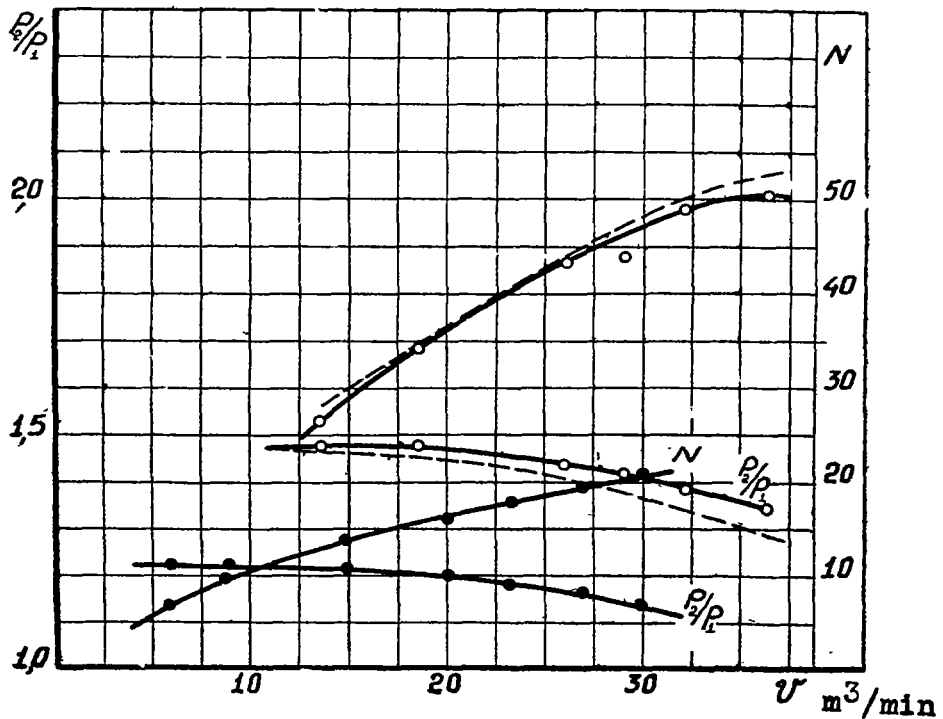


Figure 25d.- Compressor provided with vaneless diffuser.

NASA Technical Library



3 1176 01441 5047